Enhanced neurogenic biomarker expression and reinnervation in human acute skin wounds treated by electrical stimulation

DOI:
10.1016/j.jid.2016.09.038

Document Version
Accepted author manuscript

The Journal of Investigative Dermatology

Enhanced neurogenic biomarker expression and reinnervation in human acute skin wounds treated by electrical stimulation

Journal:	*Journal of Investigative Dermatology*
Manuscript ID	JID-2016-0422.R1
Article Type:	Original Article
Date Submitted by the Author:	n/a
Complete List of Authors:	Sebastian, Anil; University of Manchester, Institute of Inflammation and Repair Volk, Susan; University of Pennsylvania, Department of Clinical Studies--Philadelphia, University of Pennsylvania School of Veterinary Medicine Halai, Poonam; University of Manchester, Institute of Inflammation and Repair Colthurst, James; Oxford Bioelectronics, Electrical stimulation Paus, Ralf; University of Muenster, Dermatology; University of Manchester, Institute of Inflammation and Repair Bayat, Ardeshir; University of Manchester, Institute of Inflammation and Repair
Key Words:	human cutaneous wound healing, neural differentiation, electrical stimulation, reinnervation, neural crest cells

Note: The following files were submitted by the author for peer review, but cannot be converted to PDF. You must view these files (e.g. movies) online.

Supplementary Dataset 1.xlsx

Centre for Dermatological Research,
Institute of Inflammation and Repair,
University of Manchester,
Oxford Road,
Manchester. M13 9PT
England, UK.

Dr. Ardeshir Bayat
Principal Investigator/Associate Professor
Tel +44(0)161 3060607
ardeshir.bayat@manchester.ac.uk

17th August 2016

RE: MS# JID-2016-0422

TITLE: Enhanced neurogenic biomarker expression and reinnervation in human acute skin wounds treated by electrical stimulation

Dear Prof. Gilchrest,

We are writing this letter to accompany the resubmission of our above referenced manuscript. We would like to thank the Reviewers for their insightful and constructive comments and have addressed them in our revised version of the manuscript. To facilitate tracking, changes to the manuscript are highlighted in the revised document. Our point-by-point response to the Associate Editor and Reviewers' comments follows.

Associate Editor:

1. *No blocking experiments were performed to demonstrate the actual importance of the biomarkers. Only FIG4 was silenced in a neuroblastoma cell line.*

We thank the editor for this comment. Based on expression analysis from control and ES-treated wounds in human subjects, our data suggest FIG4 was induced in healing wounds in response to ES. We believe that a major strength of our work is the focus of ES effects on human tissues/cells, however, we acknowledge that working with human subjects has its limitations in mechanistic investigations. As such, blocking experiments could not be performed *in vivo.* As an alternative, complimentary approach, FIG4 silencing in human neuroblastoma cells supported our hypothesis that ES promotes restoration of neural cell integrity post-vaculogenesis and subsequent neural differentiation. Additionally, we identified FIG4 as an upstream molecule to TUBB3, which again

supported the need to silence only FIG4 in a neuroblastoma cell line which could further differentiate into neurons.

2. *Why Authors did not use a keratinocyte cell line, as FIG4 is localized in those cells?*

   We thank the Reviewer for bringing up this important point. Although FIG4 expression by keratinocytes in uninjured skin is noted in our IHC studies, ES has been shown to have an effect on TUBB3 in neural-crest derived cells and neural cells, and shown to be significantly associated with neural differentiation during the healing process. Using Ingenuity Pathway Analysis, we showed that FIG4 is an upstream molecule to TUBB3. This indicated the direct effect of FIG4 on neural-crest derived and neural cells. Therefore, in order to prove our hypothesis on the downstream effect of FIG4 in neural differentiation, we chose to investigate a specific cell line with which we could potentially differentiate to neurons in *in vitro* situation. We have made reference to the as of yet undefined mechanisms by which FIG4 may regulate keratinocyte activity and its fate in our modified Discussion (page 17, paragraph 1) and we look forward to being able to more precisely define the role of FIG4 in re-epithelization during cutaneous repair in future studies.

3. *Why does FIG4 colocalize with TUB3 in neuroblastoma and not in the skin? TUB3 and FIG4 are differentially localized, while Authors state that FIG4 is upstream of TUB3. Their correlation in the skin is unclear.*

   Thank you for your comment. In our experiments, we have investigated and focused on a wound healing scenario where maximum cellular dynamics is envisaged in the Proliferative phase compared to uninjured skin. The temporal expression of different molecules in a tissue is quite challenging to interpret during wound healing. To provide us with further information on the interactive function and specificity of molecules to one another in tissues, we performed a whole genome array and a subsequent microarray pathway analysis. Individual target proteins can interact with additional proteins to accelerate the expression of a downstream mediators, even though its own expression profile may continue to remain low in tissues. Also, we partially hypothesize contribution by paracrine signaling where extra-cellular FIG4 could also determine the expression of cellular TUBB3. Since the co-localization pattern in tissues is unclear in the current study, we performed *in vitro* experiments, primarily to show the dependency/interaction of FIG4 and TUBB3.

4. *Immunohistochemistry of FIG4 is of poor quality and not convincing.*

   Thank you for your comment. Because of the nature of the tissues, antibodies and staining mechanisms the provided images are the best we could achieve from our IHC staining. Moreover, punch biopsies were also used for investigating the numerous biomarkers related to neural differentiation (and that too in

triplicates), antibody standardising experiments and few other non-reported markers in the current study. However, with the images and detailed explanations in the amended manuscript, hope the reviewer now finds the data convincing.

5. *Page 10: last paragraph and last two sentences are not supported by data. Evidence is indirect. Authors should block NGF function first. In addition, Authors should have looked at the effect of NGF on K and fibroblast, also involved in wound healing*

Thank you for your comment. We have now amended the sentence to fit our findings, on page 11, paragraph 1.

6. *Page 8, last sentence of the first paragraph..." Notably, ES induces...." makes little sense to me, and it is not based on presented results.*

Thank you for your comment. The authors agree that this sentence does not contribute to the interpretation of the data and has thus been removed.

Minor:

1. *Page 5, second paragraph. "Cell-associated neural differentiation...." Sentence is incomplete: either a verb is lacking or english is wrong.*

   Thank you for your comment. We have now amended the sentence according to the reviewer's suggestion on page 5, paragraph 2.

2. *Page 5, second paragraph and first two lines of page 6 contain very old references both on TUBB3 and NGF. NGF functions and signaling are much more complex than those reported by Authors. Authors should take into consideration the effects of NGF on K and fibroblast in relation to wound healing.*

   Thank you for the comment. We have primarily investigated the role of ES on neural-crest derived cells and neural cells in differentiation and re-innervation, and have now added references of relevance that will make the article more informative to the reader. In addition, NGF plays a key role in keratinocyte differentiation and fibroblast proliferation in different stages of healing. We have now amended the introduction to reflect this.

   Please see changes on page 5, paragraph 2.

Reviewer comments:

Reviewer 1:

Comments to the Author

The manuscript "Enhanced neurogenic biomarker expression and reinnervation in human acute skin wounds treated by electrical stimulation" by Sebastian et al. aims to elucidate the effect of electrical stimulation (ES) on the reinnervation of cutanous wounds. The authors have previously published that ES promotes cutaneous wound healing and in this study they aim to determine a more mechanistic reason for this improvement in healing. The study is well thought out and provides some very elegant data to support reinnervation as a contributing factor in the improved healing seen with ES treatment. Whilst very good I feel there are a few things that could improve the study. I have the following comments:

We thank reviewer 1 for the favorable comments and appreciate the suggestions which we feel have improved our manuscript.

Major corrections:

1. *Is neuronal signaling essential for wound healing? Diabetic patients often suffer from neuropathy and poor cutaneous healing, but there are many other confounding factors in these patients. What happens in the absence of the nerves only? Has anyone ever, for example, looked at nerve ablation prior to cutaneous wound healing? Or antagonist treatment to block neuronal signaling?*

   Thank you for your comment. Innervation has been shown to be essential to optimal healing of cutaneous wounds. There is documented evidence in delayed wound healing in clinical and experimental studies of denervated tissue, which is also highlighted with the imbalance of neuromediators found in denervated disease states such as diabetes, where delayed wound healing is common. Indeed, diabetes albeit being complicated by confounding factors is a good example of where neural involvement (neuropathy) precedes the onset of wound healing problems in the form of ulcers.

   The following recent reference has now been added to the manuscript.

   Ashrafi M, Baguneid M, Bayat A. The Role of Neuromediators and Innervation in Cutaneous Wound Healing. Acta Derm Venereol. 2016 Jun 15;96(5):587-94. doi: 10.2340/00015555-2321.

   Please see changes on page 15, paragraph 1.

2. *Introduction: TUBB3 is indeed used as a marker of reinnervation of regenerating tissue, but is a pan-neuronal marker (ie. Labels sensory and motor neurons). Do*

the authors know if the nerves in the skin are only sensory (they mention sensory nerves in the discussion) or are there motor neurons involved too? Sweat glands in the skin are supplied by motor neurons of the parasympathetic branch.

Thank you for your comment. Indeed, the skin is comprised of both sensory and vasomotor nerves. TUBB3 is expressed on both motor and sensory neurons. Therefore, the TUBB3 antibody is considered a pan-neuronal marker and would not differentiate between motor and sensory neurons. Although it is beyond the scope of this paper to elaborate on the differential distribution post stimulation, we will now amend the text to refer to the fact that both sensory and motor nerves will be affected as a result of ES stimulation.

Please see changes on page 14, paragraph 1.

3. *Pg 8, line 28: What do the authors mean by "Notably, ES induced TUBB3 precedes the differences in ES mediated reinnervation of the wound, consistent with the role of TUBB3 in ES mediated neural differentiation." Since gene expression usually precedes translational changes isn't this a given? An increase in TUBB3 expression may simply precede translation of beta-III-tubulin protein, and doesn't necessarily mean differentiation is occurring.*

Thank you for your comment. As stated above, this sentence has now been removed from the text.

4. *The authors should include information in the manuscript about what PGP9.5 and substance P are and why they are of relevance to this study. As far as I understand PGP9.5 labels neuronal bodies and axons of the central and peripheral nervous system and substance P is a neuropeptide and neurotransmitter produced by keratinocytes and fibroblasts.*

Thank you for your comment. We agree that there was a need to elaborate on the rationale for examining these two markers of reinnervation in our study. In our initial ES study (Sebastian et al., 2011), SP and PGP9.5 transcripts were found to be significantly up-regulated in day 14 ES-treated wounds (60- and 30-fold respectively) and day 14 control wounds (50- and 10-fold respectively), compared to uninjured skin. This provoked the hypothesis that ES could up-regulate neural differentiation in wound healing. To investigate mechanisms by which ES induced neural differentiation and reinnervation during cutaneous wound healing, we evaluated the widely accepted reinnervation marker PGP9.5 in wound healing. We have now amended introduction to address the reviewer's suggestion.

Please see changes on page 6, paragraph 2.

5. *Pg 10, line 13: The authors state "Interestingly, the results failed to reveal any*

evidence of proliferation (as evidenced by Ki67+co-localization in gp100+ melanocytes) in the wound healing niche. Did the authors assess any other marker of proliferation (phospho-histone 3, Cyclin D1, etc)? In addition, did they consider looking at apoptosis (Caspase 3; they mention apoptosis on line 19, but don't investigate it) or senescence (p16) in the ES-treated versus non wounds?

Thank you for your comment. We have not further investigated proliferation with other biomarkers primarily because of the scarcity of healing tissue sections for performing histological experiments. Tissue sections were used for investigating the numerous biomarkers related to neural differentiation (and that too in triplicates), antibody standardising experiments and few other non-reported markers in the current study. Unfortunately, we were unable to perform further analysis to expand our studies, including potential additional mechanisms leading to an increase in melanocytes noted. The rationale to examine proliferation was guided by the literature, as most of the recent publications have used Ki67 as the standard biomarker for proliferation analysis. Nevertheless, we acknowledge that a decrease in apoptosis/senescence may account for differences in cell numbers.
This text has been amended on page 11, paragraph 1.

6. *What was the rationale for using a neuroblastoma cell line rather than a keratinocyte cell line (since the authors mention that FIG4 is produced by epidermal keratinocytes)?*

Thank you for your comment. Our *in vivo* results have shown that ES has an effect on TUBB3 in neural-crest derived cells and neural cells, and importantly, is significantly associated to neural differentiation. The Ingenuity Pathway Analysis showed that FIG4 is an upstream molecule to TUBB3. This indicated the direct effect of FIG4 on neural-crest derived and neural cells. Therefore, to understand the downstream effect of FIG4 in neural differentiation, we chose a specific cell line, which could potentially differentiate to neurons in *in vitro* situation and further prove our *in vivo* hypothesis.

7. *Pg 11, line 96: "western blot analysis of neuroblastoma cells showed significant up-regulation of Class-II phosphatidylinositol-3-kinase (PI3KII) and FIG4, post RA+BDNF+ES treatment" and Pg 12, line 12: "to understand the functional role of FIG4 gene in PIP3 pathway". Why would they investigate the PIP3 pathway? This seems like a leap into something that has not been well introduced. Please explain the rationale for looking at this pathway.*

Thank you for your comment. In the introduction, we have now stated that "*Several neural differentiation biomarkers that have been identified, including mitotic spindle components (Jouhilahti et al., 2008) to lipid membrane domains (Prinetti et al., 2001). Factor Induced Gene 4 (FIG4), a key plasma membrane protein with critical roles in phosphatidylinositol (3,4,5)-triphosphate (PI(3,4,5)P_3 or PIP_3) synthesis and neural differentiation (Winters et al., 2011), has also been*

established as a biomarker for reinnervation". Since lipid membrane domains are shown to have critical roles in neural differentiation and FIG4 is a key molecule in PIP3 lipid biosynthesis pathway (Supplementary figure S8d), we investigated the effect of ES in this pathway.

This has been further explained in the Discussion (page 17, paragraph 2) of the revised manuscript.

8. *Figure 3: Epidermal FIG4 appears to be cytoplasmic in the uninjured skin and nuclear in the injured skin (both ES-treated and untreated). Can the authors comment on this? Since the authors show that FIG4 is increased in their neuroblastoma cell line following ES does their result that knocking down FIG4 (siRNA) actually improves ES-induced production of NeuN and TUBB3 come as a surprise? Please discuss further.*

We thank the reviewer for pointing out this interesting finding that we had noted, but had neglected to raise in our discussion. Please find included in the results (page 12, paragraph 1) and discussion (page 17, paragraph 2) of this revised manuscript. Although beyond the scope of this manuscript, this is a potential topic of further ES research.

The Ingenuity Pathway Analysis showed that FIG4 is an upstream molecule to TUBB3. The up-regulation of FIG4 post-ES in FIG4 knocked down neuroblastoma cell line could also lead to up-regulation of TUBB3 and several neural differentiation processes. This is an additional support to the existence of FIG4-TUBB3 axis in wound healing. Here, we have shown the advantage of ES to act on specific molecules that could potentially determine cell fate and neural differentiation.

9. *What is the clinical outcome of such a study? Can the authors suggest how such a therapy may be of benefit to patients with chronic non-healing wounds (diabetic ulcers, venous ulcers, pressure sores)? Since these patients suffer from a proteolytic wound environment, reinnervation of such tissue may have little to no effect on healing outcome.*

Thank you for your comment. The finding of this study has potential clinical implication for targeted device-assisted acceleration of process of re-innervation in cutaneous repair post-injury. ES therapy may be of direct benefit in prevention or in addition to conventional therapy (debridement and skin substitute replacement) to patients with chronic non-healing wounds (diabetic ulcers, venous ulcers, pressure sores).

Please see changes at the end of the abstract and on page 18, paragraph 1.

Minor corrections:

1. *In the abstract the authors state that TUBB3 marks melanocytes in the skin. TUBB3 also marks cutaneous nerves since it's a pan-neuronal marker. Please rephrase this to include this information in the abstract.*

   Thank you for your comment. The manuscript abstract has been amended following reviewer's suggestion.

2. *Page 5, line 47 "recent reports" Is 1998 really considered as recent?*

   We thank the reviewer for pointing out this inconsistency.

   Thank you for your comment. The manuscript has been amended following reviewer's suggestion.

3-5. Minor grammatical errors. Page 10, line 39: Post-injury rather than post injury; Pg 8, line 28: ES-mediated rather than ES mediated; Pg 15, line 53: post-ES rather than post ES.

We thank the reviewer for pointing out these grammatical errors, which have now been carefully reviewed and edited the document to ensure similar errors do not remain.

5. *In addition, the manuscript would be benefitted by more extensive proof-reading to check the grammar is correct (in many places the word "the" is missing; for example pg 15, line 38 "Subsequent enhancement in melanogenesis is a secondary effect of either increase of melanocytes or promoting melanogenesis in individual cells, supplying the regenerating epidermis with sufficient melanin").*

   Thank you for your comment. The manuscript has now been carefully reviewed and amended.

6. *The positive foci in Figure 1H (arrows) are really small and very difficult to see, can the authors increase magnification or have a separate panel with more magnified images? In addition, it would be advantageous to have what the red stain is included on the image itself, rather than simply in the legend.*

   Thank you for your comment. The figure has been amended following reviewer's suggestion.

7. *The images in Figure 3A appears to be rete ridges of human skin – what is the densely cellular structure in the middle of the image for Non-ES treated?*

   Thank you for your comment. This also illustrates NGF expression in non-ES treated tissues.

8. *Figure S8C: what are the four bars per gene target? Can the authors include the key on the figure rather than in the legend?*

   Thank you for your comment. The figure has now been amended following reviewer's suggestion.

9. *How many times were the in vitro neuroblastoma experiments performed?*

   Thank you for your comment. The *in vitro* neuroblastoma experiments were performed three times, and each time in triplicates.

10. *Discussion: What do the authors mean by "Reinnervation has been shown to be inevitable for healing without formation of ulcers or scars" Do you mean reinnervation is essential for efficient healing? Please rephrase.*

    Thank you for your comment. This has now been amended on page 15 paragraph 1.

12. *"several lines of evidence have provided mechanistic insights into accelerated neural differentiation and regeneration" – Such as? Please cite such studies.*

    Thank you for your comment. The discussion has been amended (page 15 paragraph 1) following reviewer's suggestion.

13. *The authors note in the discussion that "Shibazaki et al., had noted that TUBB3 expression was cell-cycle dependent and is mediated by the binding of RE-1-silencing transcription factor (REST) to RE-1 element, which is present in the first intron of TUBB3 gene (Shibazaki et al., 2012). Therefore, alterations in REST-TUBB3 axis could potentially cause differential expression of TUBB3." Since they discuss it did the authors investigate REST in their model?*

    Thank you for your comment. We have not investigated REST in the current research. The aim of this section is to give a background on the molecular mechanisms leading to differential expression of TUBB3 and also to introduce as a potential topic to explore further in ES-mediated wound healing. Investigating the molecular mechanisms is beyond the scope of this research paper.

14. *What were the ages/gender of the 4 participants used for the microarray study?*

    The four participants of the microarray study were all British Caucasions: two males (aged 28 and 30) and two females (aged 26 and 28). This is information can be found in the Supplementary Table S1.

Enhanced neurogenic biomarker expression and reinnervation in human acute skin wounds treated by electrical stimulation

Anil Sebastian[1], Susan W. Volk[2], Poonam Halai[1], James Colthurst[3], Ralf Paus[4,5], Ardeshir Bayat[1]

[1] Plastic Surgery Research Group, Dermatology Research Centre, Institute of Inflammation & Repair, Faculty of Medical and Human Sciences, University of Manchester, UK

[2] Section of Surgery, Department of Clinical Studies, University of Pennsylvania School of Veterinary Medicine, Philadelphia, USA

[3] Oxford Bioelectronics, Abingdon, UK

[4] Hair Follicle Biology Research Group, Dermatology Research Centre, Institute of Inflammation & Repair, Faculty of Medical and Human Sciences, University of Manchester, UK

[5] Department of Dermatology, University of Muenster, Germany

Corresponding Author:

Dr. Ardeshir Bayat,

Plastic & Reconstructive Surgery Research Group,

Dermatology Research Centre,

Institute of Inflammation & Repair,

Faculty of Medical and Human Sciences,

Stopford building, University of Manchester,

Oxford Road, Manchester, M13 9PT. UK

Email: ardeshir.bayat@manchester.ac.uk

Tel: +44 (0)161 306 5177

Keywords: electrical stimulation, human cutaneous wound healing, reinnervation, neural differentiation biomarker, TUBB3, FIG4

Short running title: Electrical stimulation enhances reinnervation

List of abbreviations

BDNF	Brain-derived neurotrophic factor
CK20	Cytokeratin 20
DW	Degenerate Waves
ES	Electrical stimulation
FIG4	Factor Induced Gene 4
IHC	Immunohistochemistry
LAMP2	Lysosomal-associated membrane protein 2
MAPK	Mitogen-activated protein kinase
NGF	Nerve growth factor
PGP9.5	Protein gene product 9.5
PI(3)P	Phosphatidylinositol 3-phosphate
$PI(3,5)P_2$	Phosphatidylinositol (3,5)-biphosphate
$PI(3,4,5)P_3$ or PIP_3	Phosphatidylinositol (3,4,5)-triphosphate
$PI(4,5)P_2$	Phosphatidylinositol (4,5)-biphosphate
PI3KII	Class-II phosphatidylinositol-3-kinase
PTEN	Phosphatase and tensin homolog
qRT-PCR	Quantitative real time PCR
RA	Retinoic acid
REST	RE-1 silencing transcription factor
SP	Substance P
siRNA	Single interference RNA
TUBB3	Class III β-tubulin

Abstract

Electrical stimulation (ES) is known to promote cutaneous healing, however its ability to regulate reinnervation remains unclear. Firstly, we show that ES treatment of human acute cutaneous wounds (n=40) increased reinnervation. Next, to define neurophysiological mechanisms through which ES impacts repair, microarray of wound biopsies was performed on days 3, 7, 10 and 14 post-wounding. This identified neural differentiation biomarkers Class III β-tubulin (TUBB3; melanocyte development and neuronal marker) and its upstream molecule Factor Induced Gene 4 (FIG4; phosphatidylinositol (3,5)-bisphosphate 5-phosphatase) as significantly up-regulated post-ES treatment. To demonstrate a functional ES-TUBB3 axis in cutaneous healing, we showed increased $TUBB3^{+}$ melanocytes and melanogenesis plus FIG4 and nerve growth factor expression, suggesting higher cellular differentiation. In supporting this role of ES to regulate neural-crest derived cell fate and differentiation *in vivo*, knock down of FIG4 in neuroblastoma cells resulted in vaculogenesis and cell degeneration, while ES treatment post FIG4-siRNA transfection enhanced neural differentiation, survival and integrity. Further characterisation showed increased $TUBB3^{+}$ and $PGP9.5^{+}$ Merkel cells during *in vivo* repair, post-ES. We demonstrate that ES contributes to increased expression of neural differentiation biomarkers, reinnervation and expansion of melanocyte and Merkel cell pool during repair. Targeted ES-assisted acceleration of healing has significant clinical implications.

.

Introduction

Reinnervation of cutaneous wounds is temporally regulated by molecular and biochemical cues during the processes of neurogenesis, synaptogenesis, and subsequent organisation of the nervous tissue (1, 2). Furthermore, spatial regulation of reinnervation of the neodermis and epidermis involves neural differentiation and synthesis of functional neuropeptides (3). During reinnervation, the central trunk of individual nerve fibres terminates in the dermis. Subsequent branches end in the dermis (4) or extend into the overlying epidermis (5). Mechanisms regulating epidermal reinnervation, particularly the spatiotemporal regulation of proteins which guide neural differentiation, remain ill-defined.

Neural differentiation is characterised by early neurite outgrowth (6), which is required for reinnervation. Several biomarkers for neural differentiation have been identified, including mitotic spindle components (7) and lipid membrane domains (8). Microtubule protein- Class III β-tubulin (TUBB3) has been classified as a neural-specific differentiation marker (9) of reinnervation in tissue regeneration (10), although at least one report suggests expression by non-neural cell types (11). Factor Induced Gene 4 (FIG4), a key plasma membrane protein with critical roles in phosphatidylinositol (3,4,5)-triphosphate ($PI(3,4,5)P_3$ or PIP_3) synthesis and neural differentiation (12), has also been established as a biomarker for reinnervation. Of particular relevance for reinnervation following cutaneous injury, nerve growth factor (NGF; key molecule in cell migration (13)) has also been shown to modulate gene expression associated with neural differentiation in neural-crest derived cells such as epidermal melanocytes (14) and Merkel cells (15), suggesting its role in promoting epidermal reinnervation following wounding.

Therapeutic strategies that can improve physiologic reinnervation of the dermis and overlying epidermis following cutaneous injury are critical to restore nociceptive integrity and limit post-injury neuropathic pain. Several studies support the ability of ES to induce reinnervation of human tissues, particularly muscle (16, 17); however, assessments have been largely based upon functional outcomes with much less attention focused on mechanisms by which these more favourable functional outcomes are achieved. ES induction of neuronal tubulin components, neurofilament 200 and *c-fos* gene expression have been implicated as mechanisms mediating neurite outgrowth and differentiation in chick embryos (18) and rats (19); however similar mechanistic studies examining reinnervation of human tissues in response to ES are lacking. Specifically, a gap in knowledge remains regarding its effect on reinnervation of human skin post-injury, despite the fact that ES has been shown to promote cutaneous wound repair in both animal models (20, 21) and humans (22).

In our initial study examining the effects of ES on human cutaneous wound healing, we identified enhanced angiogenesis and re-epithelialisation in human cutaneous wounds (23). In addition, expression of Substance P (SP; neurotransmitter) and Protein Gene Product 9.5 (PGP9.5; pan-neuronal marker) were found to be significantly up-regulated on day 14 post-injury (50 and 10 fold respectively) in non-treated wounds, compared to uninjured skin. ES-treatment further increased expression of these markers (60 and 30 fold respectively, compared to unwounded skin) at that time point. This provoked the hypothesis that ES could up-regulate neural differentiation processes in wound healing. To explicitly understand the role of ES in reinnervation during repair, temporal examination of neuronal marker expression and quantification of nerve fibers in healing human cutaneous wounds was performed (days 3, 7, 10 and 14 post-injury). We demonstrate that ES increases neural

differentiation and reinnervation in healing human cutaneous wounds and elucidate key neural differentiation biomarkers differentially expressed in response to ES treatment.

Results

Reinnervation and neuropeptide synthesis was up-regulated in ES treated wounds

Temporal punch biopsies from ES-treated and non-ES-treated wounds undergoing spontaneous healing were obtained from the upper inner arm of 40 healthy volunteers on days 3, 7, 10 and 14, following the previously published experimental design (23) (Supplementary Information). Initial expression analyses for potential biomarkers associated with ES induced reinnervation identified a significant increase in PGP9.5 transcripts in ES-treated wounds compared to control wounds (non-ES-treated wounds) at day 14 post-injury (Fig. S1a). Corresponding PGP9.5 protein expression in day 14 ES-treated wounds was also significantly upregulated compared to control wounds, reaching levels seen in uninjured skin (Figures 1a and b). A trend for earlier induction of PGP9.5 (day 7) by ES was noted but was not significant. A progressive increase in $PGP9.5^{+}$ nerve fibers within healing wounds was noted over time with significant increases seen in ES-treated wounds by day 14 post-injury compared to control wounds (Figures 1c and d; Fig S1b). In support of ES-mediated wound reinnervation, we also noted an increase in SP expression (Fig. 1e and f) and number of SP^{+} cells in wounded human skin (Fig. 1g and h, S2), with significant increases noted in ES treated wounds compared to the control wounds ($P < 0.05$) by day 14 post-injury.

TUBB3 was up-regulated in ES-treated wounds

To identify targets of ES in reinnervation, we performed whole genome transcriptional profiling using microarrays of 1) uninjured skin, 2) control wounds and 3) ES-treated wounds (wounds were assessed on days 3, 7, 10 and 14 post-injury). Class III β-tubulin (TUBB3)(24, 25), a neural differentiation as well as melanocyte-associated gene, was identified as one of

the most highly up-regulated gene (highest fold change between ES-treated and uninjured skin) in electrically stimulated wounds on healing day 14 (ES14) compared to uninjured skin and control wounds on day 14 post-injury (C14) (Fig. 2a, Dataset S1 from microarray). Subsequent qRT-PCR analysis confirmed up-regulation of intra-cutaneous TUBB3 transcription ($P < 0.05$) in ES and corresponding control wounds on day 10 and 14 post-wounding (Fig S3a) and a significant induction of TUBB3 associated with ES treatment at day 10 and 14 (~ 70% (ES10 vs C10) and 28% (ES14 vs C14), respectively). Western blot analysis and immunolocalization of TUBB3 in wounds also showed corresponding significant increases in the percentage of $TUBB3^+$ cells in day 10 and 14 ES-treated wounds compared to controls (Fig. S3b-f, Fig. 2b and c).

In addition to quantitative differences noted in TUBB3 expression between uninjured skin, control and ES-treated wounds, spatial differences in TUBB3 protein distribution in wounds were also noted. In normal healthy skin, TUBB3-like immunoreactivity was seen in isolated cells scattered along stratum basale, in addition to few intradermal cells (Fig. 2c). TUBB3 was observed in differentiating epidermal layers in the centre of healing wound (Fig. S3d). However, in the wound edge and the flanking neodermis, TUBB3 was scattered haphazardly in stratum basale cells with $TUBB3^+$ dendritic-like structures branching out to the upper layers of the epidermis (Fig. 2c). Protein results confirmed significant up-regulation ($P < 0.05$) of TUBB3 expression in ES treated wounds compared to non-treated healing wounds (~ 67% and 34% more cells were $TUBB3^+$ in ES10 and ES14 respectively, compared to the corresponding control wounds; Fig. 2b and c, Fig. S3e). In wound granulation tissue, TUBB3 expression was mostly restricted to stellate and spindle-shaped cells (presumptive fibroblasts/myofibroblasts) and occasional cells lining neo-capillaries (Fig. S3f).

ES expands the pool of melanocytes, up-regulates TUBB3 expression in melanocytes and promotes melanogenesis in cutaneous healing

In order to further characterise the role of TUBB3 in wound healing, we examined melanocyte TUBB3 expression in human cutaneous wounds. Although TUBB3 has been shown to regulate melanocyte developmental lineage (26), the effect of ES on melanocyte-associated genes and gene products has not been previously reported to our knowledge. Here, we show that ES treatment significantly increased expression of the melanocyte-lineage specific antigen (gp100) over control wounds (ES14 vs C14, $P < 0.05$; Fig. 2d). Although gp100 expression was found to be present in both the dermis and epidermis of healing wounds, the predominant population of $gp100^+$ cells localised to the epidermis of ES-treated wounds compared to relatively fewer $gp100^+$ cells in control wounds (Fig S4a). Co-immunostaining of TUBB3 with gp100 revealed that ES treatment up-regulated the number of intra-epidermal TUBB3/gp100 double-positive cells ($P < 0.05$; Fig. 2e and f, Fig. S4a). Given the fact that TUBB3 is an active component of microtubule tracks which transport melanin-containing melanosomes packed in mature melanocytes (26), we next investigated the role of ES in stimulating intra-epidermal melanogenesis using quantitative Masson-Fontana histochemistry (Fig. S4b and c). The results indicate that ES promotes TUBB3 expression outside the developing nervous system and upregulates melanogenesis, suggesting that ES may determine the extent of re-pigmentation in healing human skin.

Absence of proliferating melanocytes in healing wounds and up-regulated nerve growth factor expression in ES treated wounds

To elucidate mechanisms by which ES increased numbers of melanocytes during cutaneous wound repair, we examined proliferation in $gp100^+$ cells in human cutaneous wounds.

Interestingly, the results failed to reveal any evidence of proliferation in $gp100^+$ cells (as evidenced by $Ki67^+$ co-localization in $gp100^+$ melanocytes) in the wound healing niche (Fig. S5), suggesting that the increased number of melanocytes post-ES were due to enhanced intra-cutaneous differentiation and migration of resident precursor cells, such as melanoblasts, diminished apoptosis, a decrease in senescence may account for differences in cell numbers, or a combination of these mechanisms. Therefore, to further define the effect of ES on melanocyte differentiation, we examined neurotrophic protein epidermal nerve growth factor (NGF) expression in control and ES-treated wounds. NGF has previously been correlated to higher chemotaxis and dendricity of melanocytes *in vitro* (14), as well as to higher innervation density in various tissues (27). We found that ES-treated wounds showed significant up-regulation of NGF mRNA (Fig. S6a) and protein expression (immunohistochemistry (IHC) and Western blot analyses; Fig. 3a - d, Fig. S6b), compared to control wounds. This result suggests that ES enhances melanocyte differentiation in human skin post-injury partly through its ability to up-regulate NGF expression.

ES up-regulates FIG4 expression and enhances differentiation in a human neuroblastoma cell line

Having observed enhanced expression of neural differentiation genes following cutaneous injury *in vivo*, we investigated whether ES can promote neural differentiation *in vitro*. Further analysis of microarray data from our human cutaneous wounds revealed up-regulation of another neural differentiation biomarker, Factor Induced Gene 4 (FIG4; phosphatidylinositol (3,5)-bisphosphate 5-phosphatase) (12), in ES14 compared to C14 wounds (Dataset S1 from microarray). Moreover, Ingenuity Pathway Analysis following microarray suggested that FIG4 is an upstream signalling molecule to TUBB3. The up-regulation of FIG4 expression in

ES wounds was confirmed by transcript analysis (Fig. S7a), IHC ($P < 0.05$, ES10 vs C10 and ES14 vs C14; Fig. 3e and f, Fig. S7b) and western blot analyses ($P < 0.05$, ES7 vs C7 and ES14 vs C14; Fig. 3g and h). In uninjured skin, FIG4 expression was found to be restricted to differentiating keratinocytes (cytoplasmic) and occasional scattered cells in the dermis. In contrast, during the repair process, $FIG4^+$ cells were found more widely distributed throughout the granulation tissue and the neoepidermis (nuclear localization in cells) (Fig. S7b).

In order to assess whether ES could directly induce FIG4 expression during neural differentiation, we analysed its expression in SHSY5Y human neuroblastoma cells cultured under differentiation conditions using retinoic acid (RA) and brain-derived neurotrophic factor (BDNF) as previously described (28). As anticipated, differentiation using RA+BDNF promoted upregulation of both NeuN, a predominant post-mitotic neural nuclei marker (Fig. S8a) and FIG4 expression (Fig. S8b) in $TUBB3^+$ cells. To determine whether ES could accentuate induction of neural differentiation biomarkers, we also subjected the cells to ES (1 hour/day for 10 days) whilst they were treated with RA+BDNF. The applied electric field (100 mV/mm) corresponds to the endogenous "current of injury" prevailing in cutaneous wound healing during initiation of granulation tissue, fibroplasia, wound contraction and neovascularization (29, 30). qRT-PCR indicated FIG4 mRNA expression was increased on the 10^{th} day of RA+BDNF+ES treatment compared to RA+BDNF treatment alone ($P < 0.05$, Fig. S8c). Moreover, western blot analysis of neuroblastoma cells showed significant up-regulation of Class-II phosphatidylinositol-3-kinase (PI3KII) and FIG4, post RA+BDNF+ES treatment ($P < 0.05$, increase of ~ 77% and ~ 43%, respectively; Fig. 4a and b).

Next, to understand the functional role of FIG4 gene in PIP_3 pathway (Fig. S8d), FIG4 was knocked down in neuroblastoma cells by siRNA transfection (Fig. S8e and f). Intracellular vacuologenesis was observed 3 days post transfection (Fig. S8g). Positive immunostaining of these vacuoles for lysosomal-associated membrane protein 2 (LAMP2) suggest that these represent late-stage endosomes (31) (Fig. S8h).

Next, we investigated whether FIG4 siRNA transfected cells were capable of neural differentiation and whether ES could affect the process. For this, following FIG4 siRNA transfection, we subjected cells to 1) RA+BDNF and 2) RA+BDNF+ES treatments. Interestingly, ES treatment of FIG4 siRNA-transfected cells grown under differentiation conditions increased nuclear NeuN, FIG4 and TUBB3 expressions (Fig. S8i and j) and decreased LAMP2 expression (Fig. S8k), compared to non-ES-treated cells. qRT-PCR analysis revealed 2-fold increase in FIG4 mRNA expression post-ES treatment (Fig. S8l), which corroborated with western blot analysis (Fig. 4c and d). FIG4 was the only protein that was up-regulated by ES treatment in both mRNA and protein analyses. Next, to assess cell integrity of differentiating cells by RA+BDNF alone treatment post-FIG4 siRNA treatment, cells were subjected to a single course of ES on the final day of RA+BDNF addition. Here, all cells were lysed within 35 minutes of ES (Video S1). In contrast, cells exposed to ES throughout differentiation (RA+BDNF+ES) post-FIG4 siRNA treatment survived (Video S2). This result indicated the potential of ES to restore the integrity of neural cells post-vacuologenesis and subsequent differentiation process.

ES enhances TUBB3 expression in Merkel cells during reinnervation of cutaneous wounds *in vivo*

Given the induction of innervation by ES and the spatial distribution of TUBB3$^+$ cells during healing, we pursued the novel hypothesis that ES could promote TUBB3 expression in Merkel cells. These neural-crest derived cells attached to sensory nerve fibres can be identified by the Merkel cell-selective cytokeratin CK20. TUBB3 is expressed on both motor and sensory neurons and the skin is compromised of both sensory and vasomotor nerves. Therefore, the TUBB3 antibody would not differentiate between motor and sensory neurons in the skin and as such is considered a pan-neuronal marker in the skin.

From the co-expression results, few CK20$^+$ cells in the epidermis and dermis expressed TUBB3 (Fig. S9a). However, TUBB3$^+$/CK20$^+$ cell numbers increased in the epidermis with subsequent wound healing days (Fig. 5a and b). Interestingly, ES significantly increased TUBB3$^+$/CK20$^+$ cells on healing days 10 and 14 compared to respective non-ES-treated wounds ($P < 0.05$, fold change ES10/C10 and ES14/C14 = 1.44 and 1.50 respectively; $P > 0.05$ on all other healing days). Next, to determine whether ES could induce Merkel cell reinnervation, we co-stained Merkel cells with PGP9.5. A significant increase in the percentage of PGP9.5$^+$/CK20$^+$ cells was noted in ES-treated wounds at day 14 compared to control wounds ($P < 0.05$, fold change ES14/C14 = 1.48; Fig. 5c and d, Fig. S9b). Notably, the majority of PGP9.5$^+$/CK20$^+$ cells were localised to the dermis of wound healing tissues compared to the epidermis in uninjured skin. Taken together, the data suggests enhancement of distinct sub-populations of Merkel cells (TUBB3$^+$/CK20$^+$ and PGP9.5$^+$/CK20$^+$), post-ES. Collectively, our studies suggest that ES promotes neural differentiation and reinnervation by targeting specific proteins such as TUBB3 and FIG4, during human cutaneous repair.

Discussion

Reinnervation has been shown to be essential for healing without formation of chronic ulcers or pathologic scars (32). Several studies have provided insights into mechanisms promoting accelerated neural differentiation and tissue regeneration (33, 34). In complimentary clinical and experimental studies, documented imbalances of neuromediators found in denervated tissue are associated with conditions where delayed wound healing is common. Indeed, diabetes is a good example of where neural involvement (neuropathy) precedes the onset of wound healing problems in the form of ulcers (35). However, during repair, the challenge for regenerating neurons to reach targets is counteracted by its slow rate of regeneration of 1mm/day, together with progressive loss of regenerative capacity over time and distance (36). Therefore, strategies that can accelerate neural differentiation and reinnervation hold particular promise for these problematic wounds. To our knowledge, this is the first report to quantitatively investigate reinnervation and the associated spatiotemporal induction of neural differentiation biomarkers in response to ES treatment in human cutaneous wounds. Notably, ES significantly up-regulated 1) TUBB3 in human wounds, melanocyte count, $TUBB3^{+}$ melanocytes and melanogenesis, 2) NGF in wound granulation tissue, 3) FIG4 in human wounds and *in vitro* neural differentiation and finally, 4) a fraction of $TUBB3^{+}$ Merkel cells and reinnervation in Merkel cells. Collectively, we have evidenced an increase in reinnervation in response to ES in human cutaneous wounds and provided detailed analysis of biomarker induction by ES.

Up-regulation of TUBB3 in ES-treated wounds was associated with an increase in dendritic processes of peripheral neurons in dermis and epidermis. Interestingly, Shibazaki *et al.*, had noted that TUBB3 expression was cell-cycle dependent and is mediated by the binding of

RE-1-silencing transcription factor (REST) to RE-1 element, which is present in the first intron of TUBB3 gene (25). Therefore, alterations in REST-TUBB3 axis could potentially cause differential expression of TUBB3. The presence of TUBB3 has been noted in the microtubules of keratinocytes (7) and fibroblasts (37) previously, although the physiologic significance of TUBB3 expression has been ill-defined in these cell types or in epidermal nerve fibre network formation during repair (38).

As neural-crest derived cells, melanocytes share many similarities with peripheral neurons including the presence of multiple dendritic processes, expression of similar cell surface receptors (e.g. $p75^{NTR}$ and c-Kit) and response to individual neurotrophins (39). Therefore, various pharmacological treatments have been shown to induce neurite outgrowth by over-expressing neurotrophins (40, 41). NGF, in association with ES has been reported to induce neurite outgrowth *in vitro* (6), which in part is correlated to enhanced cellular differentiation process. NGF binds to neural/neural-cell related surface receptor, Tropomyosin receptor kinase A and initiates various intracellular signalling pathways (6) leading to cell differentiation. ES enhanced NGF expression in wounds, which may explain higher chemotaxis of melanocytes from neighbouring healthy interfollicular epidermis (42). Subsequent enhancement in melanogenesis is secondary to either increasing of melanocyte numbers or promoting melanogenesis in individual cells, supplying the regenerating epidermis with sufficient melanin (43). In addition, up-regulated TUBB3 expression in melanocytes is also an indication of higher differentiation, characterised with increased dendrite formation (14) as observed in our *in vivo* results.

We also observed up-regulation of TUBB3 expression post-ES in Merkel cells which are in association with nerve terminals in this case. This increased expression of TUBB3 could promote a differentiated melanocyte lineage (44). Henceforth, this data provides further insight into possible application of ES to augment innervation in undifferentiated/immature Merkel cells in the bulge area of hair follicles. Majority of $CK20^{+}$ cells in contact with $PGP9.5^{+}$ cells were found only in the dermis. However, $TUBB3^{+}/CK20^{+}$ cells were observed in both epidermis and dermis with higher numbers in the epidermis during final healing stages. This raises the question whether Merkel cells migrate to the epidermis post-initiation of differentiation during wound healing or paradoxically, whether it is it necessary for Merkel cells to have contact guidance with nerve elements whilst undergoing differentiation.

Formation of vacuoles that express late endosome markers in response to FIG4 knock down in SHSY5Y human neuroblastoma cells in our studies is consistent with the previous work of Chow *et al.*, which showed inactivation of FIG4 and PI(5)kinase (Pikfyve) with an abrogation of phosphatidylinositol 3,5-bisphosphate ($PI(3,5)P_2$) synthesis resulted in late endosome accumulation (45, 46). The synthesis of $PI(3,5)P_2$ from phosphatidylinositol 3-phosphate (PI(3)P) requires Pikfyve for plasma membrane lipid turnover during cell differentiation (47). The reverse reaction requires $PI(3,5)P_2$ 5-phosphatase FIG4 (48) and interestingly, both the proteins for the forward and backward reactions coexist in the same protein complex (49). However, from our results, the unique specificity of ES in regulating FIG4 in this multi-complex needs further investigation. In addition, the mechanism by which FIG4 may regulate keratinocyte activity, intracellular localization and cell fate remains unknown and requires further studies to precisely define the role of FIG4 in re-epithelialization during repair.

Finally, the apparent up-regulation of neuropeptides in the granulation tissue and the temporal and spatial advancement of nerve fibres in the epidermis of ES-treated wounds suggest the effect of ES to be more proximal to sensory nerves, albeit studies continue to examine the primary target of ES. In this context, the non-invasive methodology of ES to promote neural differentiation, in addition to our data showing increased cell survival post ES of *in vitro* differentiated cells, suggests new perspectives and molecular targets for ES in tissue repair. In conclusion, our findings provide the first evidence that ES application promotes reinnervation of human skin following acute injury and up-regulates neural differentiation biomarkers while having similar effects on melanocytes and Merkel cells *in vivo*. The finding of this study has potential clinical implications for targeted device-assisted acceleration of re-innervation of cutaneous wounds post-injury. ES therapy may be of direct benefit in the prevention of chronic wound formation or as an adjuvant therapy to conventional treatment (debridement and skin substitute replacement) of chronic non-healing wounds (diabetic ulcers, venous ulcers, pressure sores).

Materials and Methods

Patient selection and recruitment

This study was conducted in accordance with the ethical principles of Good Clinical Practice and the Declaration of Helsinki. This study received ethical approval from the local research committee (Manchester, UK), and all subjects (n=40; Table S1) gave full written, informed consent.

SHSY5Y cell culture and differentiation

Human neuroblastoma SHSY5Y cells were purchased from ATCC (CRL-2266) and cell culture is explained in Supplementary information.

In vitro electrical stimulation

SHSY5Y cells were subjected to DW (Degenerate Waves) ES waveform (50) at 100 mV/mm (60 Hz).

Electrical stimulation device used on human volunteers

The electrical stimulation device used for *in vivo* ES-treated wounds was the Fenzian electrobiofeedback system (Fenzian Ltd, Hungerford, UK)(23).

Human punch biopsy collection for wound healing studies

The protocol that we adopted for *in vivo* ES studies is mentioned in our previous study (23). The detailed procedure is explained in Supplementary information.

Tissue preparation for wax-embedding, section cutting, histological staining and semi-quantitation

Tissues for wax-embedding were fixed in 10% neutral-buffered formalin (cat. F5304; Sigma-Aldrich, Dorset, UK) at 4°C and processed as described previously (22).

Microarray analysis

In microarray (n=4), normal wound healing samples were compared to ES samples on days 3, 7, 10 and 14, explained in detail in the Supplementary Information.

RNA isolation, cDNA synthesis and quantitative real time- polymerase chain reaction

For *in vivo* biopsies obtained on different days of healing, RNA isolation, cDNA synthesis, and qRT-PCR were performed as explained previously (22). RPL32 was used as the internal control and $\Delta\Delta C_T$ method was used to calculate fold change of gene expression. The primers used are detailed in Table S2.

Immunohistochemistry and immunocytochemistry

Immunohistochemical staining was performed as detailed in our previous reports (22). Tissue immunofluorescence and immunocytochemistry experiments are detailed in Supplementary Information. All antibodies and incubation parameters are detailed in Table S3.

Immunohistochemistry image analysis by Definiens software

Definiens tissue studio version 3.51 (Definiens AK, Munchen, Germany) was used to quantitate the IHC results (23), mentioned in detail in the Supplementary Information.

Western blotting

For cells: Western blotting was performed according to our previous protocol (23). 1-step nitro blue tetrazolium / S-bromo-4-chloroindoxyl phosphate (NBT/BCIP, cat. 34042; Thermo Scientific) was used to develop the blot.

For tissues: Tissues were lysed in RIPA buffer and homogenised in tissue lyser (Qiagen). They were centrifuged at 10,000 *g* for 20 min and the supernatant collected. Further protein separation and blotting were performed as explained for cell studies. Antibodies, incubation time and detection methods are detailed in Table S4.

Western blot band analysis by Image J software

Percentage of band intensity was calculated by Image J (Fiji, 1.47t, NIH, USA) analysis (23). This is further explained in Supplementary Information.

Masson-Fontana histochemistry

Quantitative melanin histochemistry by Masson–Fontana stain was performed as described in the Supplementary Information.

FIG4 siRNA transfection

SHSY5Y cells (4×10^5 cells/well) were cultured in 22 mm collagen coated cover slips in 6-well plates and transfection was carried out using siRNA complexes prepared with siPORT™ NeoFX™ Transfection Reagent (Ambion) according to manufacturer's protocol.

Microscopy and nerve fibre thickness

This was performed in NIH Image J software as described in the Supplementary Information.

Statistical analysis

Data is presented as mean +/- standard deviation from three independent experiments performed in triplicates (n=3). Statistical analysis was calculated using one way ANOVA for comparison between three groups with Turkey post-hoc test, and student's *t* test for comparison between two groups. Confidence intervals of 95% with corresponding *P* value of 0.05 were chosen throughout analysis.

Conflict of Interest

Dr James Colthurst is an employee of Oxford Bioelectronics Ltd.

Acknowledgements

We thank Miss Sara Ud-din for human punch biopsy collection and transfer, Dr. Gary Sidgwick for Human Tissue Act (HTA 2004) documentation and Professor Sylvia Paus for helpful advice and discussion regarding this manuscript.

Author contributions

AB, AS, JC conceived and designed the study; RP designed melanogenesis experiments; AS, PH performed the experiments; AS, AB, SWV, JC and RP analysed and discussed the results; AS, AB, SWV, RP wrote the manuscript.

References

1. Singer HS, Chiu AY, Meiri KF, Morell P, Nelson PG, Tennekoon G. Advances in understanding the development of the nervous system. Current opinion in neurology. 1994;7(2):153-9.
2. Pomeroy SL, Kim JY. Biology and pathobiology of neuronal development. Mental retardation and developmental disabilities research reviews. 2000;6(1):41-6.
3. Hsu YC, Li L, Fuchs E. Emerging interactions between skin stem cells and their niches. Nature medicine. 2014;20(8):847-56.
4. Karanth SS, Springall DR, Kuhn DM, Levene MM, Polak JM. An immunocytochemical study of cutaneous innervation and the distribution of neuropeptides and protein gene product 9.5 in man and commonly employed laboratory animals. The American journal of anatomy. 1991;191(4):369-83.
5. Reilly DM, Ferdinando D, Johnston C, Shaw C, Buchanan KD, Green MR. The epidermal nerve fibre network: characterization of nerve fibres in human skin by confocal microscopy and assessment of racial variations. The British journal of dermatology. 1997;137(2):163-70.
6. Chang YJ, Hsu CM, Lin CH, Lu MS, Chen L. Electrical stimulation promotes nerve growth factor-induced neurite outgrowth and signaling. Biochimica et biophysica acta. 2013;1830(8):4130-6.
7. Jouhilahti EM, Peltonen S, Peltonen J. Class III beta-tubulin is a component of the mitotic spindle in multiple cell types. The journal of histochemistry and cytochemistry : official journal of the Histochemistry Society. 2008;56(12):1113-9.
8. Prinetti A, Chigorno V, Prioni S, Loberto N, Marano N, Tettamanti G, et al. Changes in the lipid turnover, composition, and organization, as sphingolipid-enriched membrane domains, in rat cerebellar granule cells developing in vitro. The Journal of biological chemistry. 2001;276(24):21136-45.
9. Geisert EE, Jr., Frankfurter A. The neuronal response to injury as visualized by immunostaining of class III beta-tubulin in the rat. Neuroscience letters. 1989;102(2-3):137-41.
10. Knox SM, Lombaert IM, Haddox CL, Abrams SR, Cotrim A, Wilson AJ, et al. Parasympathetic stimulation improves epithelial organ regeneration. Nature communications. 2013;4:1494.
11. Luduena RF. Multiple forms of tubulin: different gene products and covalent modifications. International review of cytology. 1998;178:207-75.
12. Winters JJ, Ferguson CJ, Lenk GM, Giger-Mateeva VI, Shrager P, Meisler MH, et al. Congenital CNS hypomyelination in the Fig4 null mouse is rescued by neuronal expression of the PI(3,5)P(2) phosphatase Fig4. The Journal of neuroscience : the official journal of the Society for Neuroscience. 2011;31(48):17736-51.
13. Chen JC, Lin BB, Hu HW, Lin C, Jin WY, Zhang FB, et al. NGF accelerates cutaneous wound healing by promoting the migration of dermal fibroblasts via the PI3K/Akt-Rac1-JNK and ERK pathways. BioMed research international. 2014;2014:547187.
14. Yaar M, Grossman K, Eller M, Gilchrest BA. Evidence for nerve growth factor-mediated paracrine effects in human epidermis. J Cell Biol. 1991;115(3):821-8.
15. Vos P, Stark F, Pittman RN. Merkel cells in vitro: production of nerve growth factor and selective interactions with sensory neurons. Developmental biology. 1991;144(2):281-300.
16. Gordon T, Amirjani N, Edwards DC, Chan KM. Brief post-surgical electrical stimulation accelerates axon regeneration and muscle reinnervation without affecting the

functional measures in carpal tunnel syndrome patients. Experimental neurology. 2010;223(1):192-202.
17. Guzman-Venegas RA, Bralic MP, Cordero JJ, Cavada G, Araneda OF. Concordance of the location of the innervation zone of the tibialis anterior muscle using voluntary and imposed contractions by electrostimulation. Journal of electromyography and kinesiology : official journal of the International Society of Electrophysiological Kinesiology. 2016;27:18-23.
18. Wood M, Willits RK. Short-duration, DC electrical stimulation increases chick embryo DRG neurite outgrowth. Bioelectromagnetics. 2006;27(4):328-31.
19. Udina E, Furey M, Busch S, Silver J, Gordon T, Fouad K. Electrical stimulation of intact peripheral sensory axons in rats promotes outgrowth of their central projections. Experimental neurology. 2008;210(1):238-47.
20. Ojingwa JC, Isseroff RR. Electrical stimulation of wound healing. The Journal of investigative dermatology. 2003;121(1):1-12.
21. Kloth LC. Electrical stimulation for wound healing: a review of evidence from in vitro studies, animal experiments, and clinical trials. Int J Low Extrem Wounds. 2005;4(1):23-44.
22. Sebastian A, Syed F, Perry D, Balamurugan V, Colthurst J, Chaudhry IH, et al. Acceleration of cutaneous healing by electrical stimulation: degenerate electrical waveform down-regulates inflammation, up-regulates angiogenesis and advances remodeling in temporal punch biopsies in a human volunteer study. Wound repair and regeneration : official publication of the Wound Healing Society [and] the European Tissue Repair Society. 2011;19(6):693-708.
23. Sebastian A, Iqbal SA, Colthurst J, Volk SW, Bayat A. Electrical Stimulation Enhances Epidermal Proliferation in Human Cutaneous Wounds by Modulating p53-SIVA1 Interaction. The Journal of investigative dermatology. 2015.
24. Akasaka K, Maesawa C, Shibazaki M, Maeda F, Takahashi K, Akasaka T, et al. Loss of class III beta-tubulin induced by histone deacetylation is associated with chemosensitivity to paclitaxel in malignant melanoma cells. The Journal of investigative dermatology. 2009;129(6):1516-26.
25. Shibazaki M, Maesawa C, Akasaka K, Kasai S, Yasuhira S, Kanno K, et al. Transcriptional and post-transcriptional regulation of betaIII-tubulin protein expression in relation with cell cycle-dependent regulation of tumor cells. International journal of oncology. 2012;40(3):695-702.
26. Locher H, de Rooij KE, de Groot JC, van Doorn R, Gruis NA, Lowik CW, et al. Class III beta-tubulin, a novel biomarker in the human melanocyte lineage. Differentiation; research in biological diversity. 2013;85(4-5):173-81.
27. Korsching S, Thoenen H. Nerve growth factor in sympathetic ganglia and corresponding target organs of the rat: correlation with density of sympathetic innervation. Proceedings of the National Academy of Sciences of the United States of America. 1983;80(11):3513-6.
28. Mastroeni D, Grover A, Leonard B, Joyce JN, Coleman PD, Kozik B, et al. Microglial responses to dopamine in a cell culture model of Parkinson's disease. Neurobiology of aging. 2009;30(11):1805-17.
29. Nuccitelli R, Nuccitelli P, Ramlatchan S, Sanger R, Smith PJ. Imaging the electric field associated with mouse and human skin wounds. Wound repair and regeneration : official publication of the Wound Healing Society [and] the European Tissue Repair Society. 2008;16(3):432-41.
30. Nuccitelli R, Nuccitelli P, Li C, Narsing S, Pariser DM, Lui K. The electric field near human skin wounds declines with age and provides a noninvasive indicator of wound

healing. Wound repair and regeneration : official publication of the Wound Healing Society [and] the European Tissue Repair Society. 2011;19(5):645-55.
31. Huynh KK, Eskelinen EL, Scott CC, Malevanets A, Saftig P, Grinstein S. LAMP proteins are required for fusion of lysosomes with phagosomes. Embo J. 2007;26(2):313-24.
32. Johnson PC, Doll SC. Dermal nerves in human diabetic subjects. Diabetes. 1984;33(3):244-50.
33. Migliorini E, Grenci G, Ban J, Pozzato A, Tormen M, Lazzarino M, et al. Acceleration of neuronal precursors differentiation induced by substrate nanotopography. Biotechnology and bioengineering. 2011;108(11):2736-46.
34. Akimoto J. Photodynamic Therapy for Malignant Brain Tumors. Neurologia medico-chirurgica. 2016;56(4):151-7.
35. Ashrafi M, Baguneid M, Bayat A. The Role of Neuromediators and Innervation in Cutaneous Wound Healing. Acta dermato-venereologica. 2016;96(5):587-94.
36. Fu SY, Gordon T. Contributing factors to poor functional recovery after delayed nerve repair: prolonged denervation. The Journal of neuroscience : the official journal of the Society for Neuroscience. 1995;15(5 Pt 2):3886-95.
37. Draberova E, Lukas Z, Ivanyi D, Viklicky V, Draber P. Expression of class III beta-tubulin in normal and neoplastic human tissues. Histochemistry and cell biology. 1998;109(3):231-9.
38. Lauria G, Borgna M, Morbin M, Lombardi R, Mazzoleni G, Sghirlanzoni A, et al. Tubule and neurofilament immunoreactivity in human hairy skin: markers for intraepidermal nerve fibers. Muscle & nerve. 2004;30(3):310-6.
39. Yaar M, Park HY. Melanocytes: a window into the nervous system. The Journal of investigative dermatology. 2012;132(3 Pt 2):835-45.
40. Blesch A, Uy HS, Diergardt N, Tuszynski MH. Neurite outgrowth can be modulated in vitro using a tetracycline-repressible gene therapy vector expressing human nerve growth factor. Journal of neuroscience research. 2000;59(3):402-9.
41. Hefti F. Neurotrophic Factor Therapy for Nervous-System Degenerative Diseases. Journal of neurobiology. 1994;25(11):1418-35.
42. Chou WC, Takeo M, Rabbani P, Hu H, Lee W, Chung YR, et al. Direct migration of follicular melanocyte stem cells to the epidermis after wounding or UVB irradiation is dependent on Mc1r signaling. Nature medicine. 2013;19(7):924-9.
43. Paus R. Migrating melanocyte stem cells: masters of disaster? Nature medicine. 2013;19(7):818-9.
44. Uchigasaki S, Suzuki H, Inoue K. Merkel cells in the vellus hair follicles of human facial skin: A study using confocal laser microscopy. J Dermatol. 2004;31(3):218-22.
45. Chow CY, Zhang Y, Dowling JJ, Jin N, Adamska M, Shiga K, et al. Mutation of FIG4 causes neurodegeneration in the pale tremor mouse and patients with CMT4J. Nature. 2007;448(7149):68-72.
46. Zhang Y, Zolov SN, Chow CY, Slutsky SG, Richardson SC, Piper RC, et al. Loss of Vac14, a regulator of the signaling lipid phosphatidylinositol 3,5-bisphosphate, results in neurodegeneration in mice. Proceedings of the National Academy of Sciences of the United States of America. 2007;104(44):17518-23.
47. Gary JD, Wurmser AE, Bonangelino CJ, Weisman LS, Emr SD. Fab1p is essential for PtdIns(3)P 5-kinase activity and the maintenance of vacuolar size and membrane homeostasis. J Cell Biol. 1998;143(1):65-79.
48. Duex JE, Nau JJ, Kauffman EJ, Weisman LS. Phosphoinositide 5-phosphatase Fig4p is required for both acute rise and subsequent fall in stress-induced phosphatidylinositol 3,5-bisphosphate levels. Eukaryot Cell. 2006;5(4):723-31.

49. Dove SK, Dong K, Kobayashi T, Williams FK, Michell RH. Phosphatidylinositol 3,5-bisphosphate and Fab1p/PlKfyve underPPIn endo-lysosome function. Biochem J. 2009;419:1-13.
50. Sebastian A, Syed F, McGrouther DA, Colthurst J, Paus R, Bayat A. A novel in vitro assay for electrophysiological research on human skin fibroblasts: degenerate electrical waves downregulate collagen I expression in keloid fibroblasts. Experimental dermatology. 2011;20(1):64-8.

Figure legends

Figure 1: Increased re-innervation and neuropeptide synthesis in ES-treated wounds. **(a)** Representative western blot (WB) of PGP9.5 expression. **(b)** Quantification of PGP9.5 expression in uninjured skin and cutaneous wounds post-injury. **(c)** Quantification of immunoreactivity to PGP9.5 (% $PGP9.5^+$ area) in uninjured skin, control and ES-treated wounds. **(d)** IHC of PGP9.5 expression. **(e)** Representative WB of Substance P (SP) expression. ES14 is ES day 14, C14 is control day 14. **(f)** Quantification of % SP^+ cells in uninjured skin and cutaneous wounds 7 and 14 days post-injury. **(g)** Quantification of IHC analysis of SP expression. **(h)** Representative IHC of SP expression. Dotted lines indicate epidermal-dermal junction. Scale bar is 100 μm.

control (non-ES treated) wounds, ES treated wounds.

Indicates statistical significance; $P < 0.05$.

Figure 2: ES treatment increases TUBB3 expression in human cutaneous wounds, specifically in melanocytes. **(a)** Microarray analysis of uninjured skin (US) and ES-treated wounds on day 14 post-injury (ES14) shows up-regulation of TUBB3. **(b)** Quantification of IHC analysis of TUBB3 expression. **(c)** Representative IHC of TUBB3 expression in uninjured skin, control (non-ES-treated) and ES-treated skin wounds at day 14. **(d)** Quantification of melanocytes indicated by % $gp100^+$ cells in uninjured skin, control and ES-treated skin wounds. **(e)** Quantification of $TUBB3^+$ melanocytes. **(f)** IHC of $TUBB3^+$ melanocytes in uninjured skin, control and ES-treated skin wounds at day 14. Dotted line indicates the epidermal-dermal junction. Scale bar is 100 μm, vol represents volunteer.

control wounds, ES treated wounds.

✦ Indicates statistical significance; $P < 0.05$.

Figure 3: NGF and FIG4 expression is up-regulated in human cutaneous wounds treated with ES. **(a)** Representative IHC and **(b)** quantification of NGF expression in uninjured skin, control (non-ES-treated) and ES-treated skin wounds at day 14. **(c)** Representative WB and **(d)** quantitation of NGF expression in uninjured skin, control and ES-treated skin wounds at day 14; $P < 0.05$. **(e)** Representative IHC and **(f)** quantification of FIG4 expression in uninjured skin, control and ES treated skin wounds at day 14. **(g)** Representative WB and **(h)** quantitation of FIG4 expression in uninjured skin, control and ES-treated skin wounds at day 14. Scale bar is 100 μm.

□ control wounds, ■ ES treated wounds.

✦ Indicates statistical significance; $P < 0.05$.

Figure 4: ES treatment enhances human SHSY5Y neuroblastoma differentiation. **(a)** Representative WB and **(b)** quantitation for mediators of PIP_3 synthesis pathway in undifferentiated neurons (UDN) and neurons cultured under differentiating conditions with and without ES treatment. **(c)** Representative WB and **(d)** quantitation for mediators of PIP_3 synthesis pathway post-FIG4 siRNA treatment. DN is differentiated neurons. Scale bar is 50 μm.

□ Undifferentiated neurons, ■ RA+BDNF treated cells, ■ RA+BDNF+ES treated cells

✦ Indicates statistical significance; $P < 0.05$.

Figure 5: ES expands the pool of TUBB3^{+} Merkel cells and increases Merkel cell reinnervation during human cutaneous wound healing. **(a)** Representative IHC of TUBB3^{+} Merkel cells in uninjured skin, control (non-ES-treated) and ES-treated skin wounds at day 14. **(b)** % TUBB3^{+} Merkel (CK20^{+}) cells in uninjured skin, control and ES-treated skin wounds at days 3, 7, 10 and 14 days post-injury. **(c)** Representative IHC of PGP9.5^{+} Merkel cells in uninjured skin, control and ES-treated skin wounds at day 14. **(d)** % PGP9.5^{+} Merkel (CK20^{+}) cells in uninjured skin, control and ES-treated skin wounds at days 3, 7, 10 and 14 days post-injury. Scale bar is 100 μm.

□ control wounds, ■ ES treated wounds.

✦ Indicates statistical significance; $P < 0.05$.

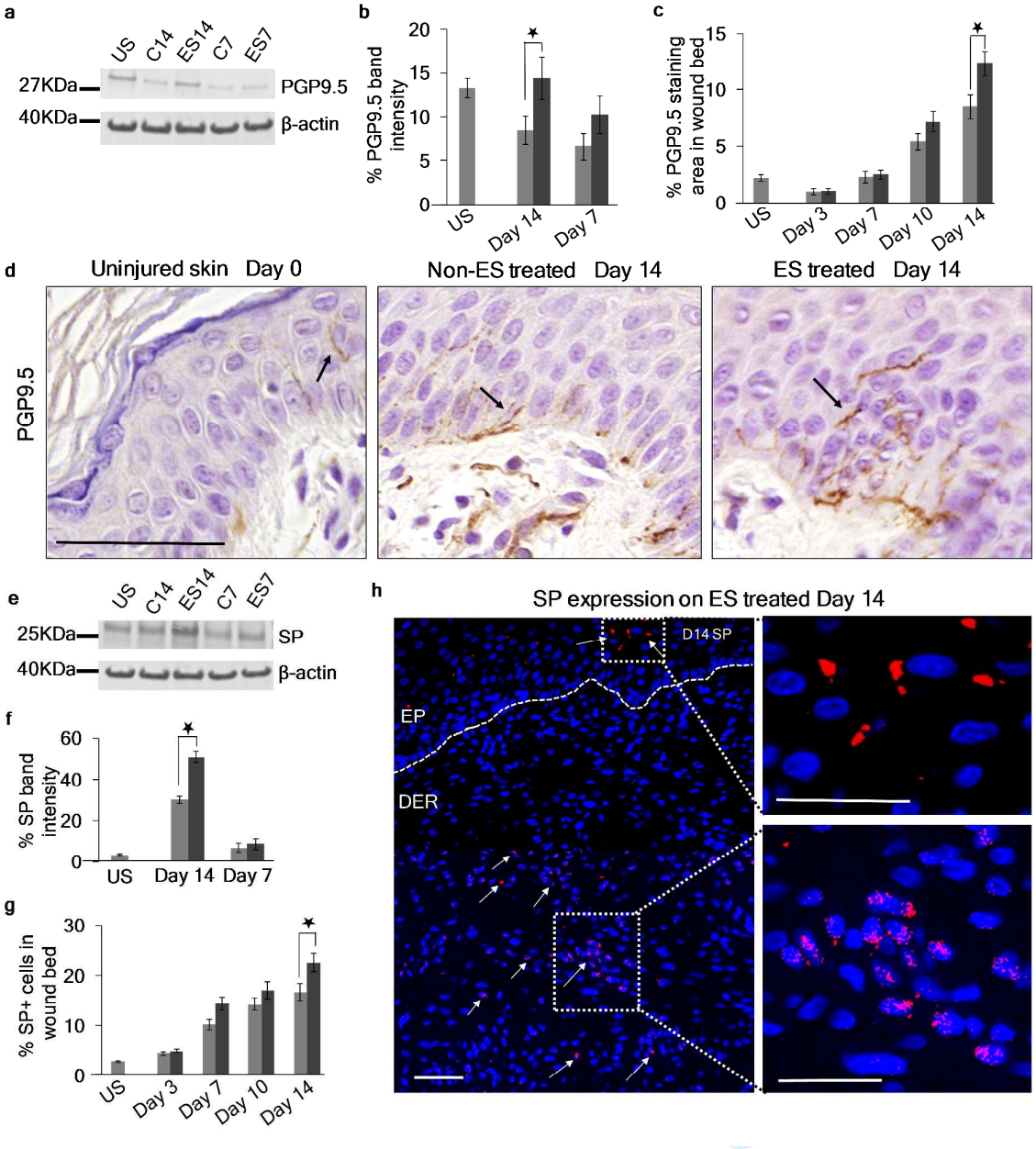
a
US
C14
ES14
C7
ES7
27KDa
40KDa
PGP9.5
β-actin
b
% PGP9.5 band intensity
US
Day 14
Day 7
c
% PGP9.5 staining area in wound bed
US
Day 3
Day 7
Day 10
Day 14
d
Uninjured skin Day 0
Non-ES treated Day 14
ES treated Day 14
PGP9.5
e
25KDa
SP
f
% SP band intensity
g
% SP+ cells in wound bed
h
SP expression on ES treated Day 14
D14 SP
EP
DER

Figure 1

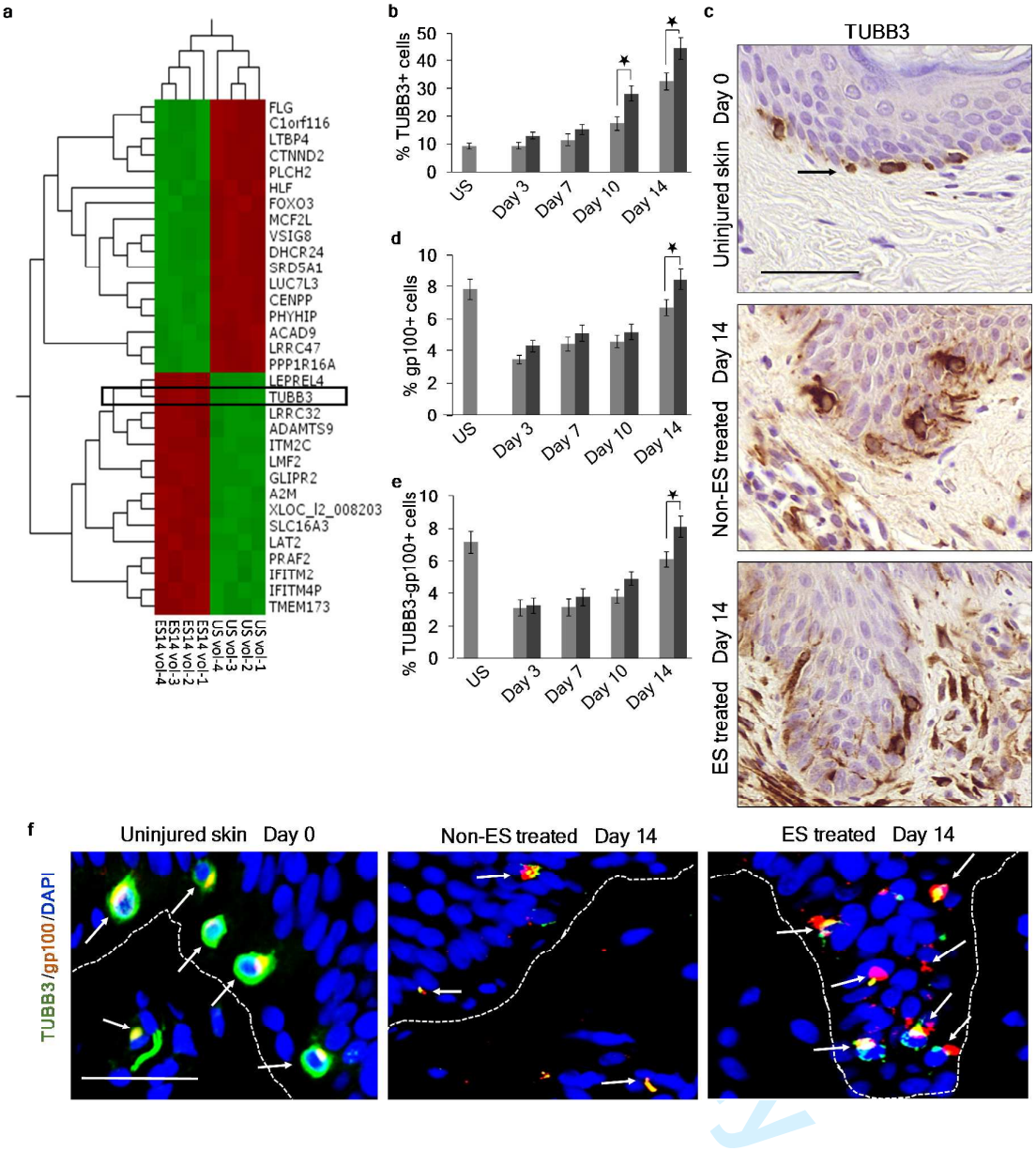
a
FLG
C1orf116
LTBP4
CTNND2
PLCH2
HLF
FOXO3
MCF2L
VSIG8
DHCR24
SRD5A1
LUC7L3
CENPP
PHYHIP
ACAD9
LRRC47
PPP1R16A
LEPREL4
TUBB3
LRRC32
ADAMTS9
ITM2C
LMF2
GLIPR2
A2M
XLOC_l2_008203
SLC16A3
LAT2
PRAF2
IFITM2
IFITM4P
TMEM173
US vol-1
US vol-2
US vol-3
US vol-4
ES14 vol-1
ES14 vol-2
ES14 vol-3
ES14 vol-4
b
% TUBB3+ cells
US
Day 3
Day 7
Day 10
Day 14
d
% gp100+ cells
e
% TUBB3-gp100+ cells
c
TUBB3
Uninjured skin Day 0
Non-ES treated Day 14
ES treated Day 14
f
Uninjured skin Day 0
Non-ES treated Day 14
ES treated Day 14
TUBB3/gp100/DAPI

Figure 2

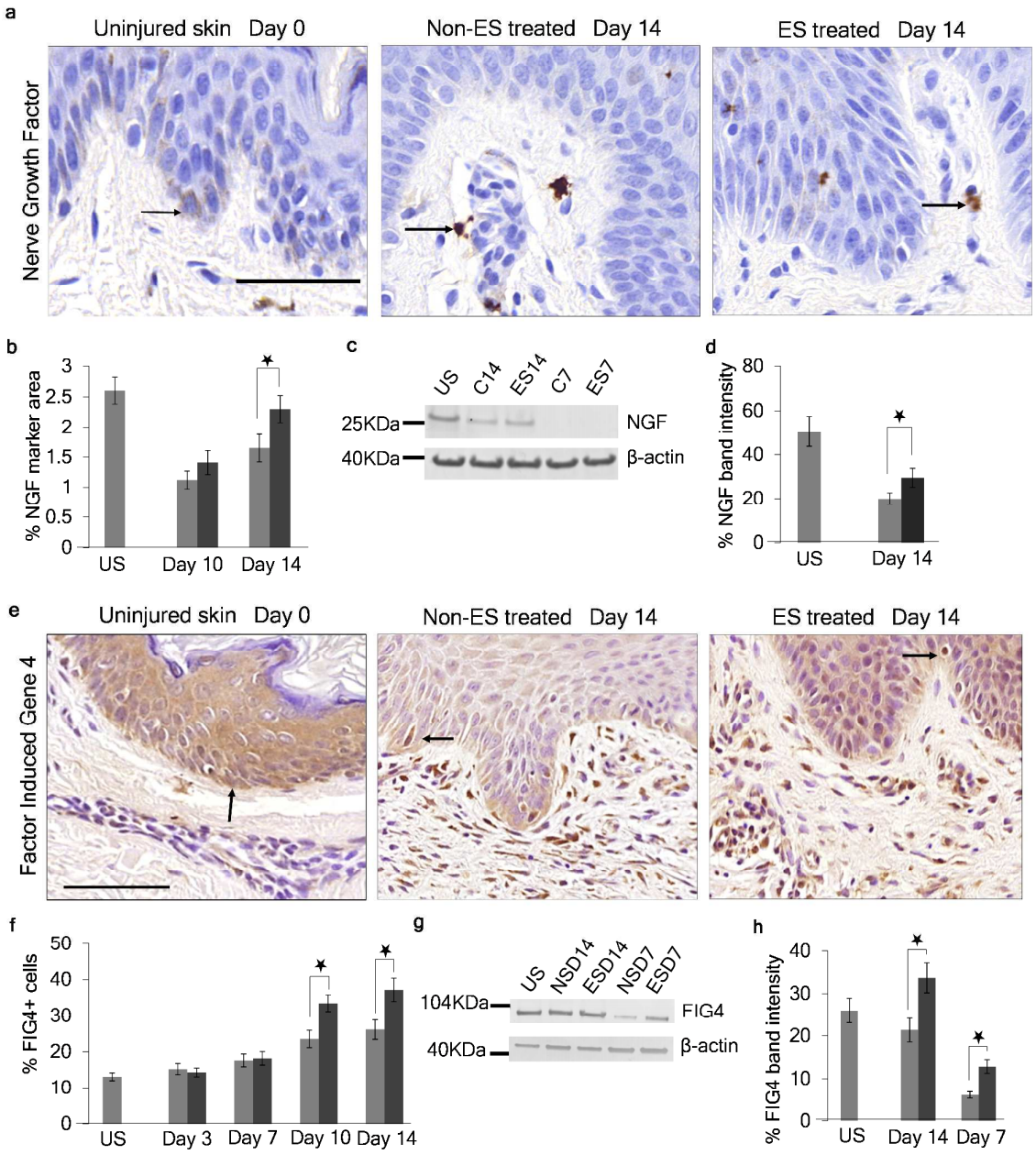
a
Uninjured skin Day 0
Non-ES treated Day 14
ES treated Day 14
Nerve Growth Factor
b
% NGF marker area
US
Day 10
Day 14
c
US
C14
ES14
C7
ES7
25KDa
NGF
40KDa
β-actin
d
% NGF band intensity
US
Day 14
e
Uninjured skin Day 0
Non-ES treated Day 14
ES treated Day 14
Factor Induced Gene 4
f
% FIG4+ cells
US
Day 3
Day 7
Day 10
Day 14
g
US
NSD14
ESD14
NSD7
ESD7
104KDa
FIG4
40KDa
β-actin
h
% FIG4 band intensity
US
Day 14
Day 7

Figure 3

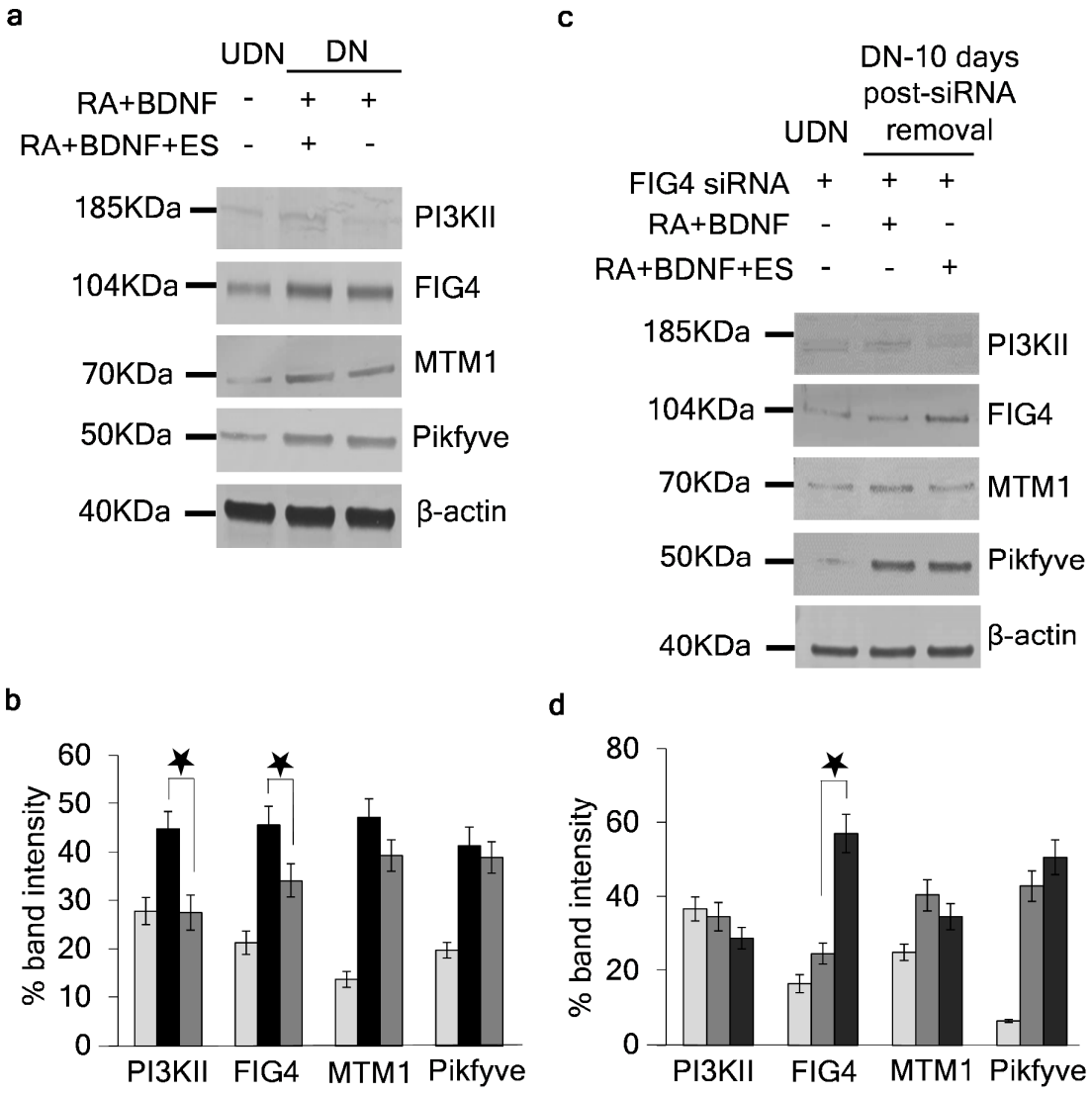
a
UDN
DN
RA+BDNF - + +
RA+BDNF+ES - + -
185KDa
PI3KII
104KDa
FIG4
70KDa
MTM1
50KDa
Pikfyve
40KDa
β-actin
c
DN-10 days post-siRNA removal
UDN
FIG4 siRNA + + +
RA+BDNF - + -
RA+BDNF+ES - - +
185KDa
PI3KII
104KDa
FIG4
70KDa
MTM1
50KDa
Pikfyve
40KDa
β-actin
b
% band intensity
60
50
40
30
20
10
0
PI3KII
FIG4
MTM1
Pikfyve
d
% band intensity
80
60
40
20
0
PI3KII
FIG4
MTM1
Pikfyve

Figure 4

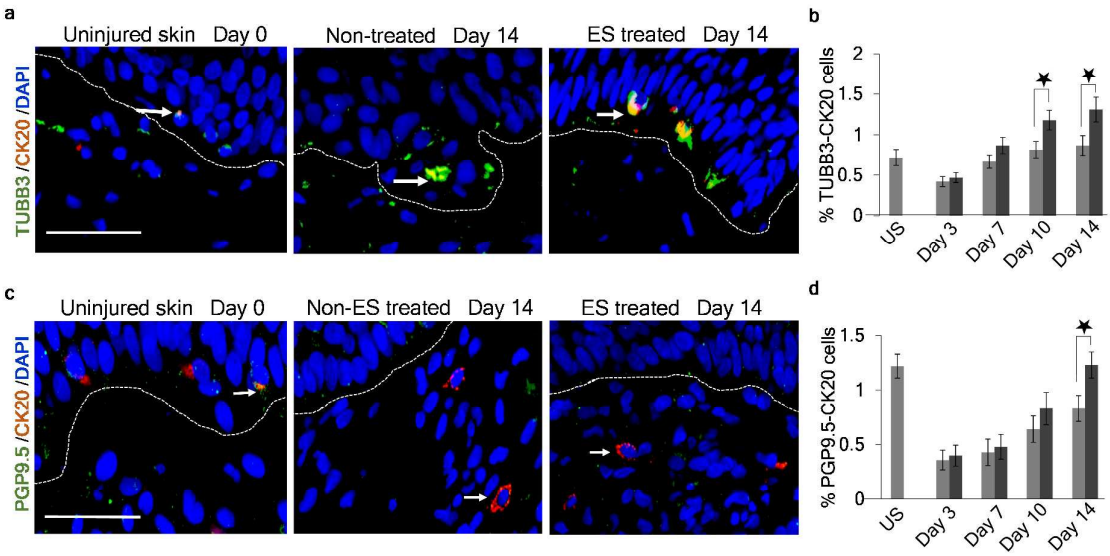

Figure 5

Supplementary information

Enhanced neurogenic biomarker expression and reinnervation in human acute skin wounds treated by electrical stimulation

Anil Sebastian[1], Susan W. Volk[2], Poonam Halai[1], James Colthurst[3], Ralf Paus[4,5], Ardeshir Bayat[1]

[1] Plastic Surgery Research Group, Dermatology Research Centre, Institute of Inflammation & Repair, Faculty of Medical and Human Sciences, University of Manchester, UK

[2] Section of Surgery, Department of Clinical Studies, University of Pennsylvania School of Veterinary Medicine, Philadelphia, USA

[3] Oxford Bioelectronics, Abingdon, UK

[4] Hair Follicle Biology Research Group, Dermatology Research Centre, Institute of Inflammation & Repair, Faculty of Medical and Human Sciences, University of Manchester, UK

[5] Department of Dermatology, University of Muenster, Germany

Corresponding Author:

Dr. Ardeshir Bayat,

Plastic Surgery Research Group,

Dermatology Research Centre,

Institute of Inflammation & Repair,

Faculty of Medical and Human Sciences,

Stopford building, University of Manchester,

Oxford Road, Manchester, M13 9PT. UK

Email: ardeshir.bayat@manchester.ac.uk

Tel: +44 (0)161 306 5177

SUPPLEMENTARY FIGURES

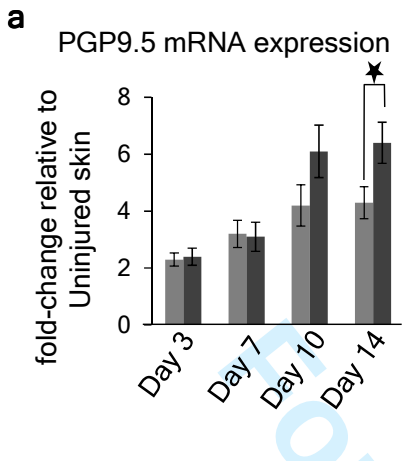

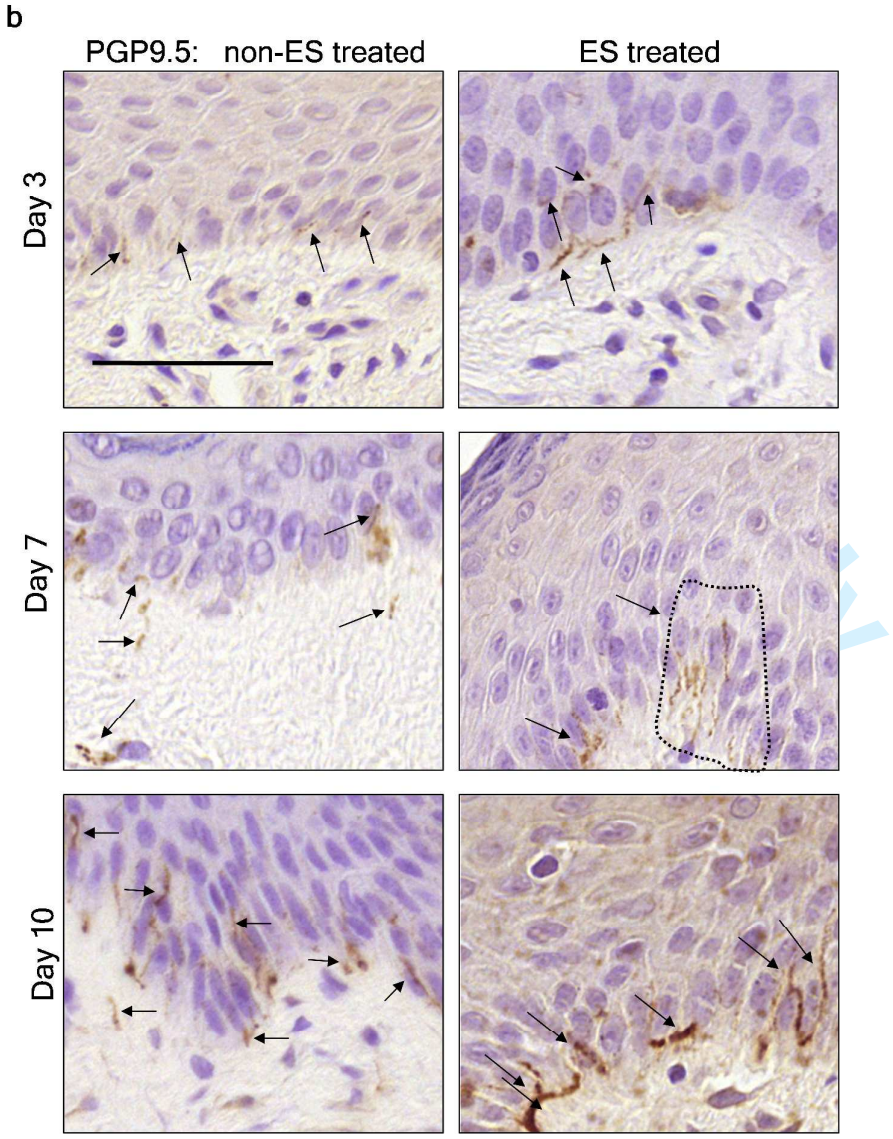

Figure S1. PGP9.5 (reinnervation analysis) in human acute cutaneous wounds. **(a)** Quantification of immunohistochemistry **(**IHC) for PGP9.5 showed higher protein expression in ES14 wounds compared to C14 wounds. **(b)** IHC of PGP9.5 expression. In the epidermis, weaker PGP9.5 signals were detected initially on healing day 3, which got stronger by day 14. Images are from the edge of the healing wound. Scale bar is 100 μm.

☐ control (non-ES treated) wounds, ■ ES treated wounds.

✦ Indicates statistical significance; $P < 0.05$.

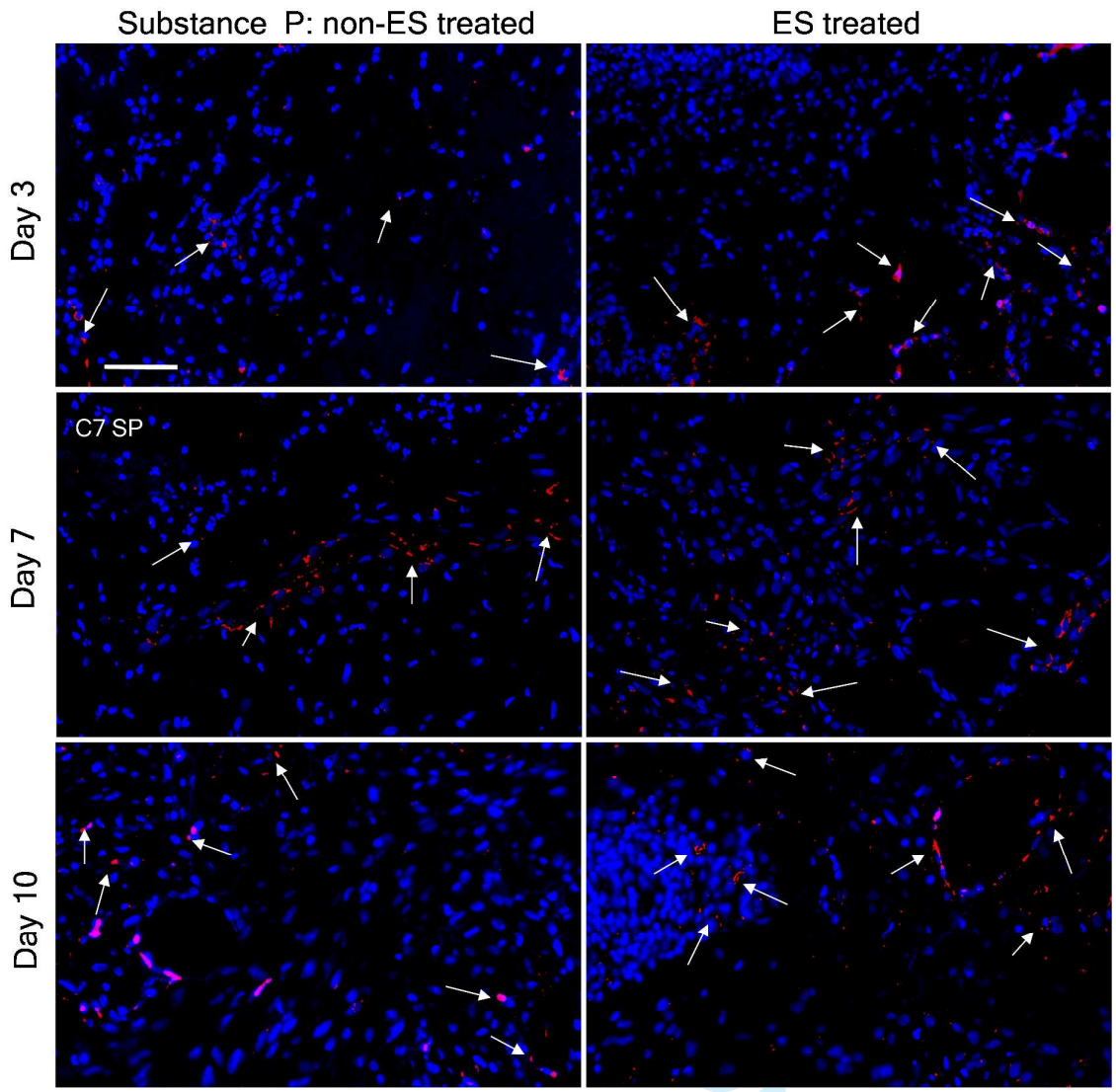
Substance P: non-ES treated
ES treated
Day 3
Day 7
Day 10
C7 SP

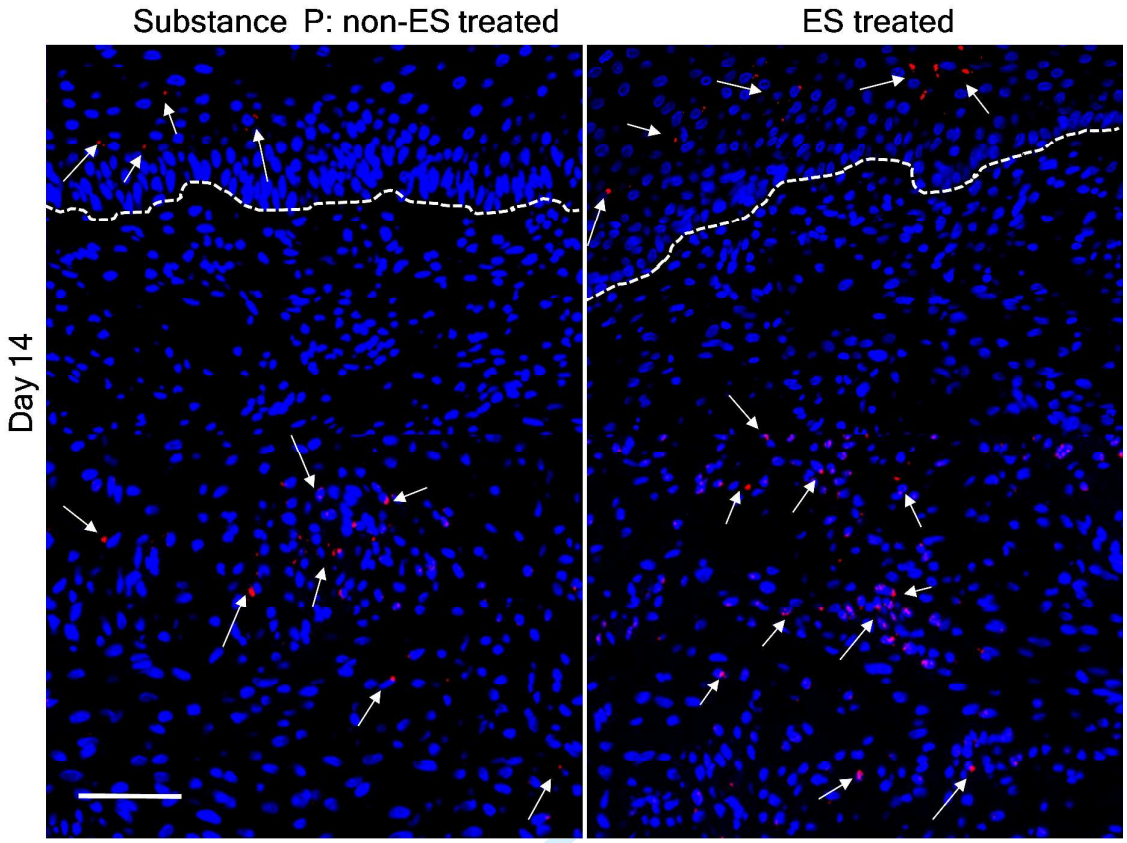

Figure S2. Substance P (SP; neuropeptide expression) in human acute cutaneous wounds. IHC of SP expression. Similar to PGP9.5 expression, expression of SP was weak till day 10 in the epidermis of healing wounds. Images are till healing day 10 from the reforming dermis, however on day 14, expression was both in the epidermis and dermis of the wound. Scale bar is 100 μm.

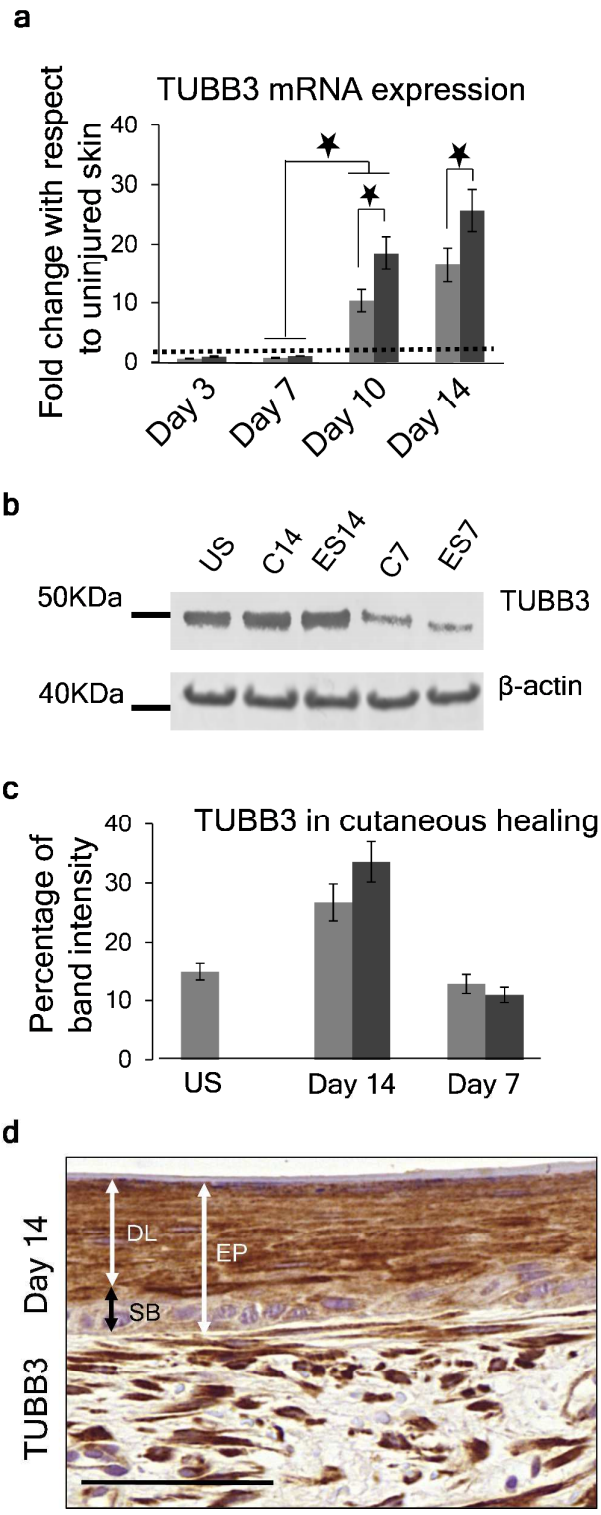

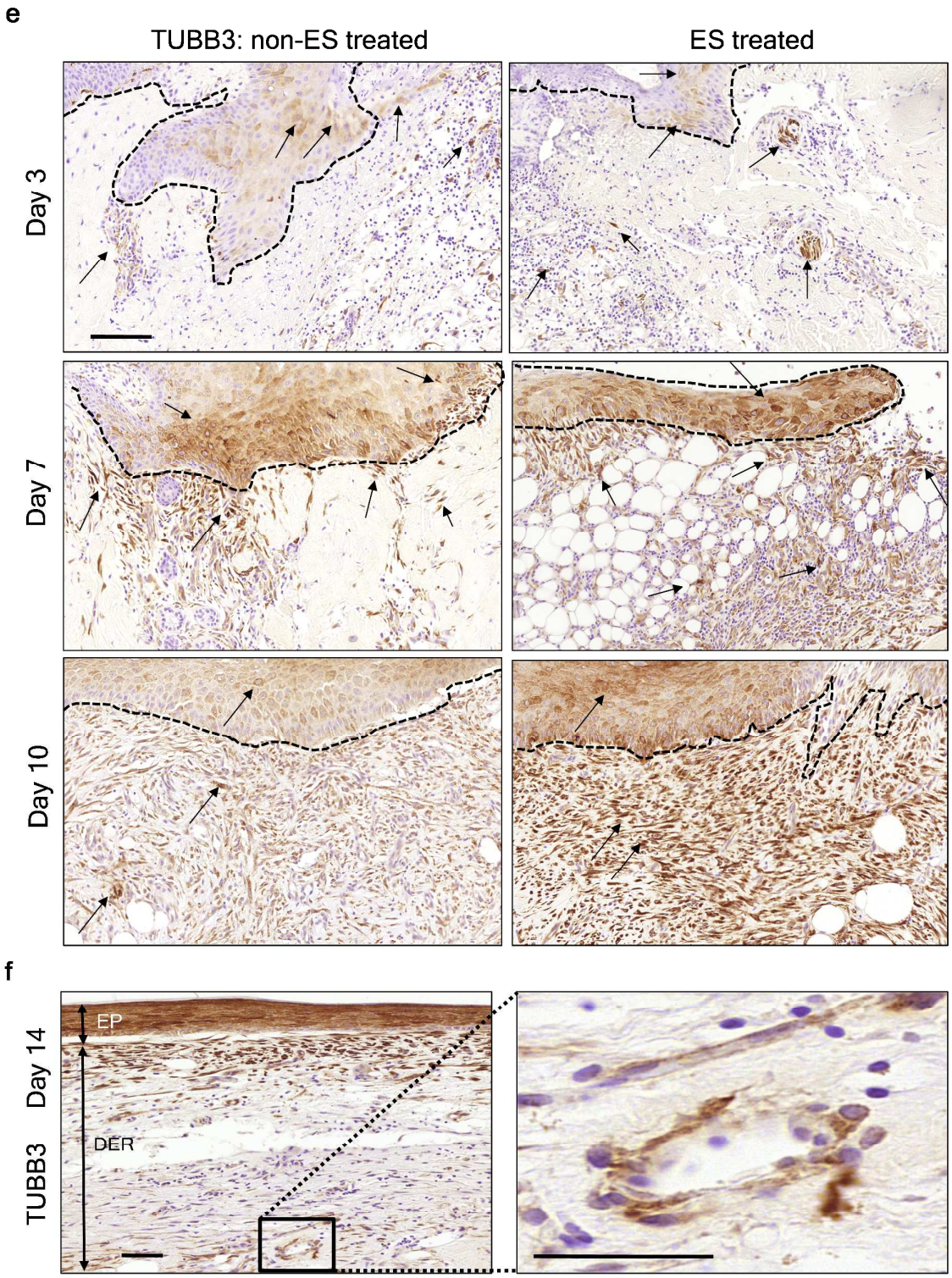
e
TUBB3: non-ES treated
ES treated
Day 3
Day 7
Day 10
f
TUBB3 Day 14
EP
DER

Figure S3. IHC images of TUBB3 expression in healing wounds. **(a)** qRT-PCR of TUBB3. **(b)** Western blotting of TUBB3 on days 7 and 14. **(c)** Quantification of TUBB3 Western blot band intensities. **(d)** TUBB3 expression in the wound centre (a representative image of healing on day 14). **(e)** IHC of TUBB3 expression. Up-regulated TUBB3 expression was observed in ES treated cutaneous wounds compared to non-ES treated healing. Dotted lines indicate epidermal-dermal junction. **(f)** TUBB3 expression in the wound dermal compartment, especially staining neo-capillaries (a representative image of healing on day 14). Scale bar is 100 μm. US is uninjured skin.

control (non-ES treated) wounds, ES treated wounds.

✦ Indicates statistical significance; $P < 0.05$.

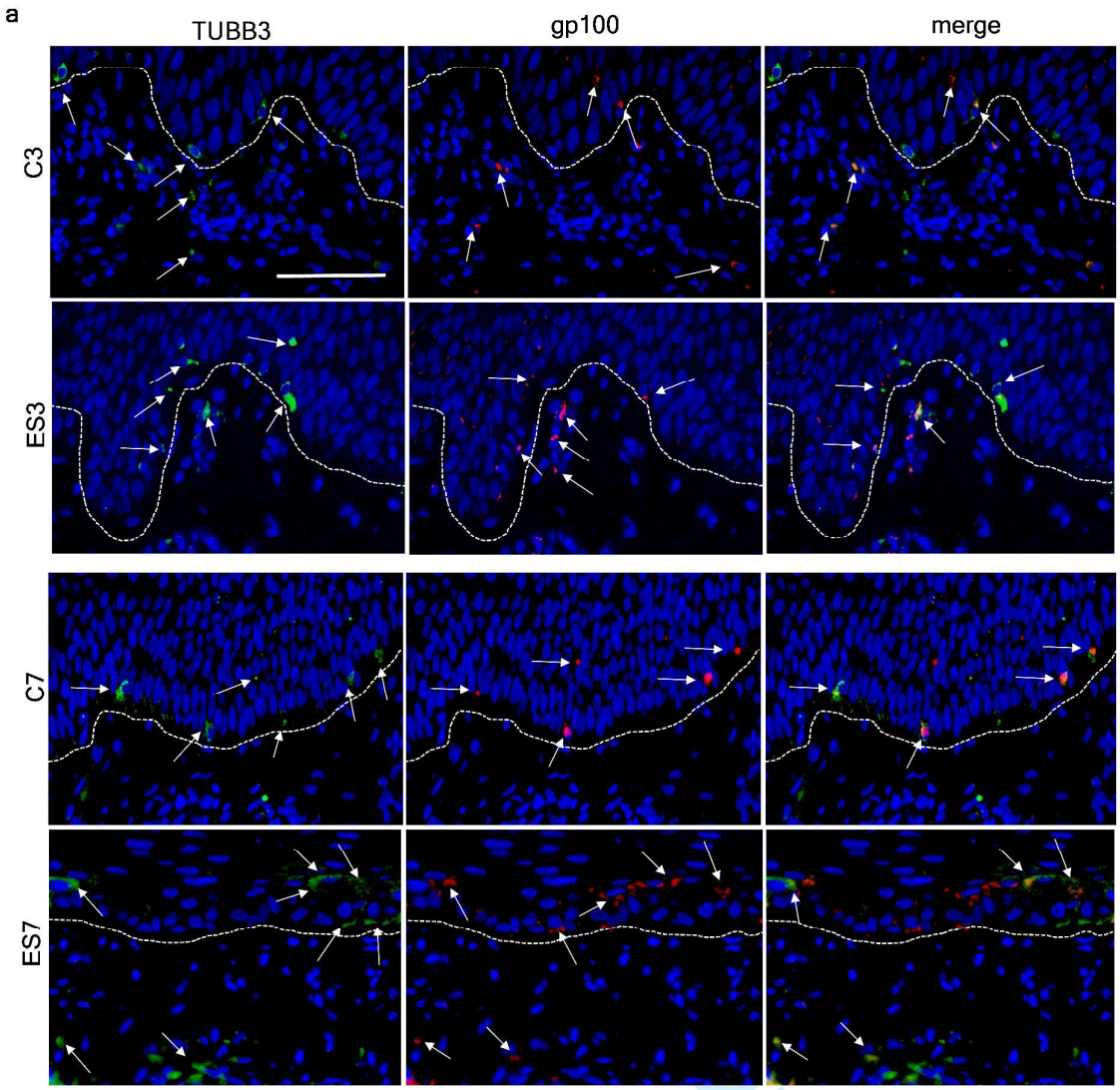

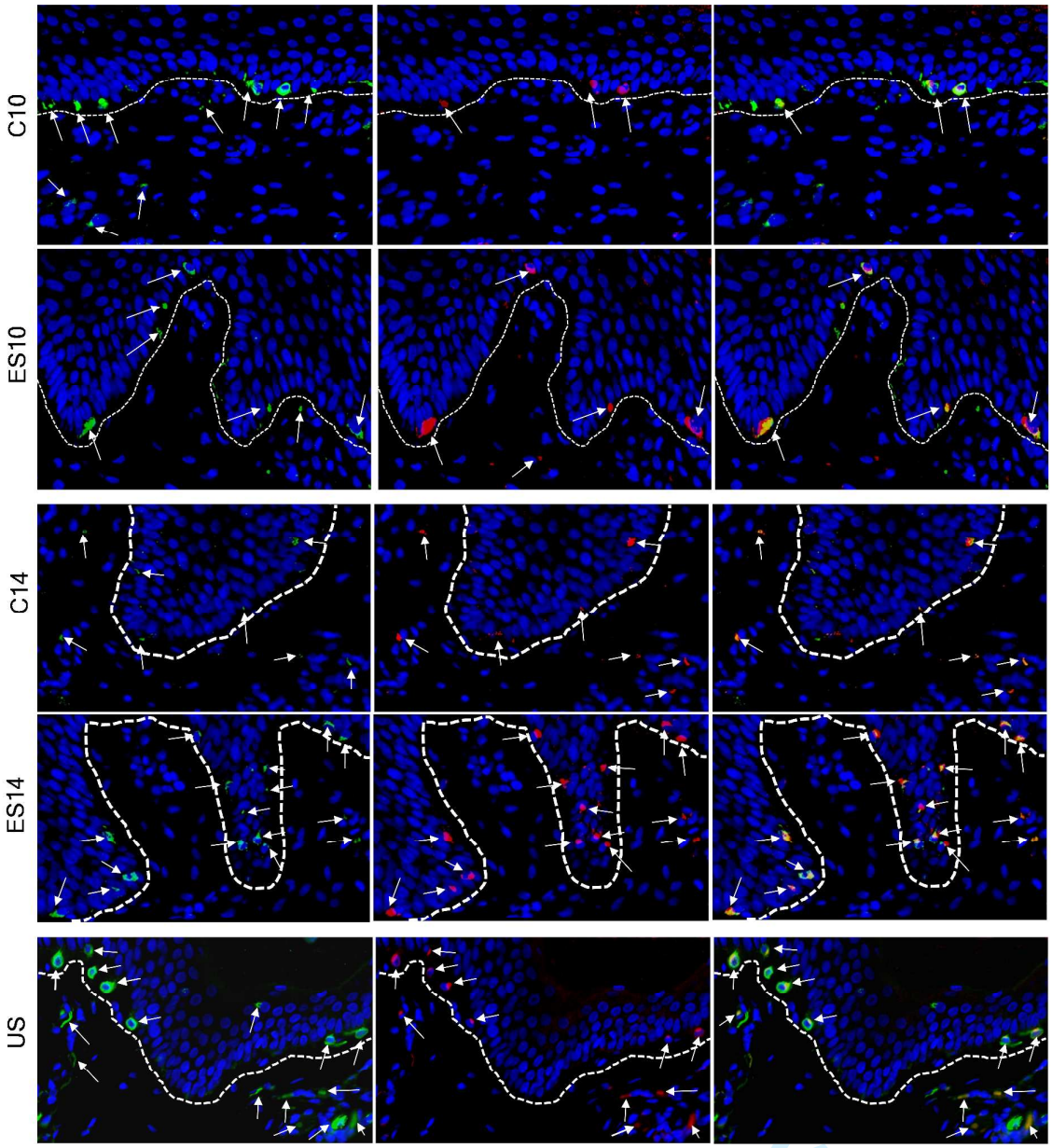
C10
ES10
C14
ES14
US

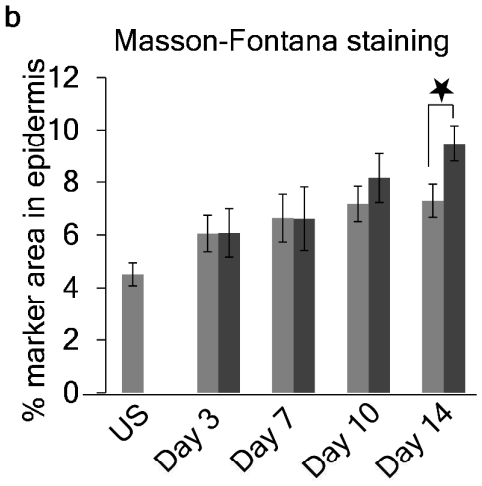

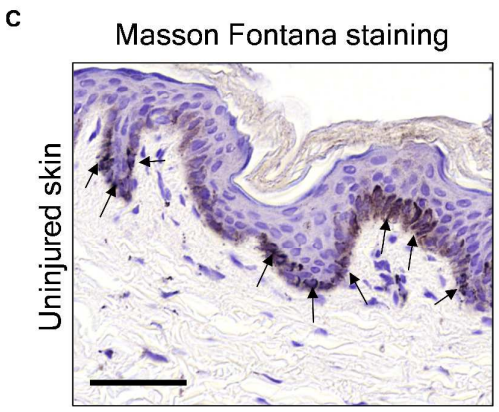

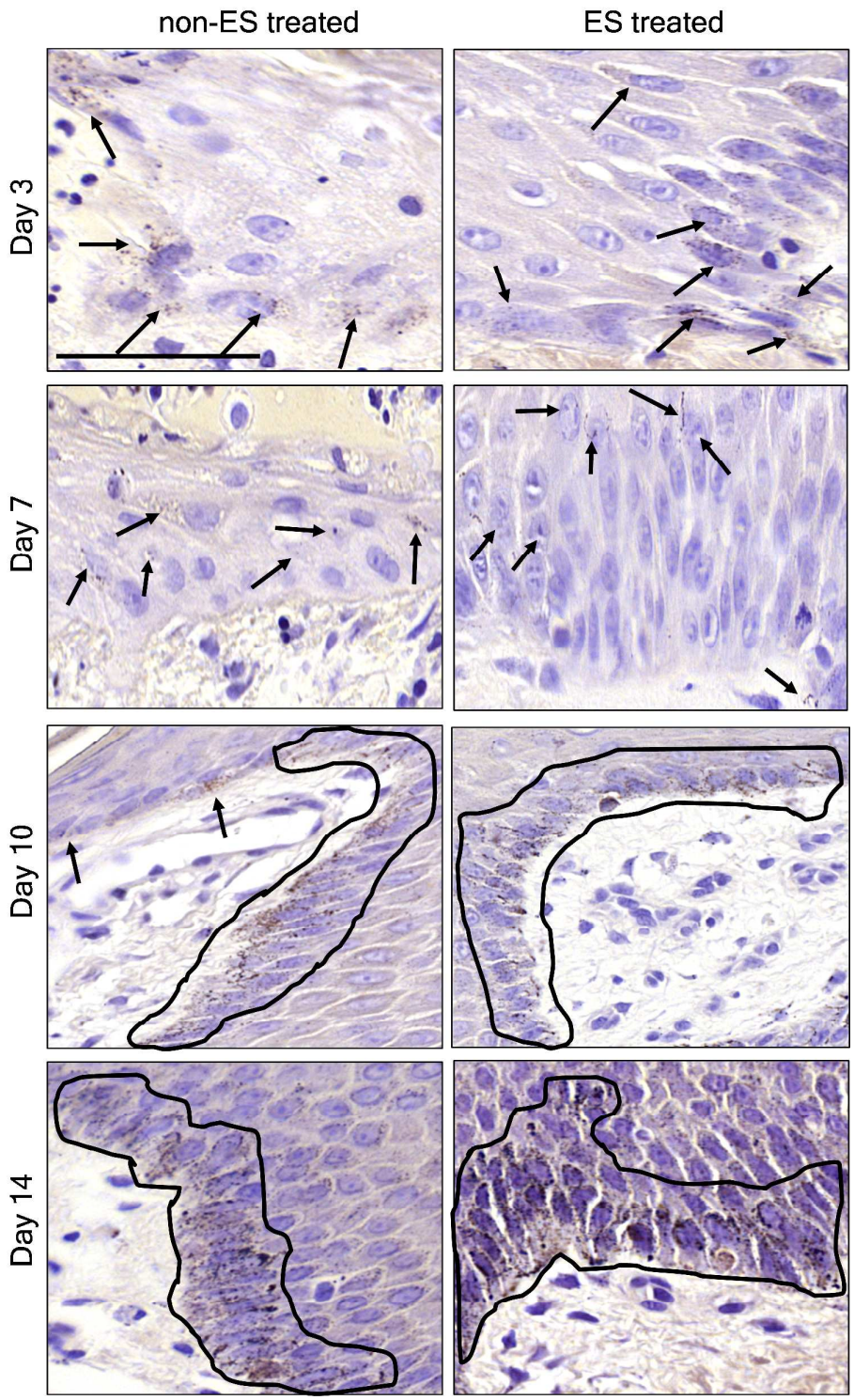
non-ES treated
ES treated
Day 3
Day 7
Day 10
Day 14

Figure S4. ES up-regulates TUBB3 expression and enhances melanogenesis in healing human skin wounds. **(a)** Co-expression of TUBB3/gp100 showed up-regulation of $TUBB3^{+}/gp100^{+}$ cells in the epidermis of ES treated wounds compared to non-ES treated wounds. Dotted lines indicate epidermal-dermal junction. **(b)** Quantitative analysis of Masson-Fontana histochemistry. **(c)** Melanogenesis analysis by Masson-Fontana histochemistry showed up-regulation in basal layer cells of healing human epidermis post-ES. Area within the marked space indicates melanogenesis. Scale bar is 100 μm. US is uninjured skin.

□ control (non-ES treated) wounds, ■ ES treated wounds.

✦ Indicates statistical significance, $P < 0.05$.

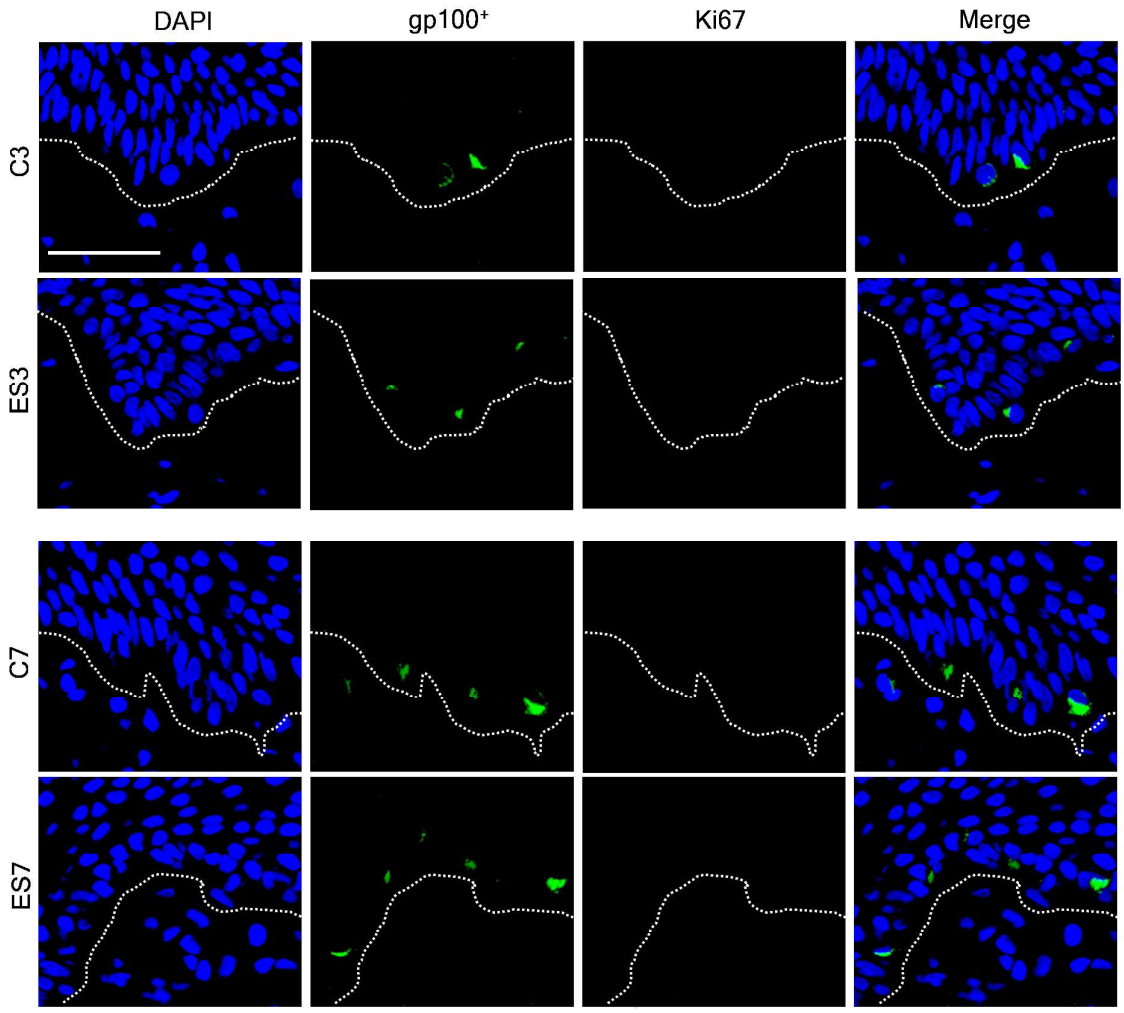

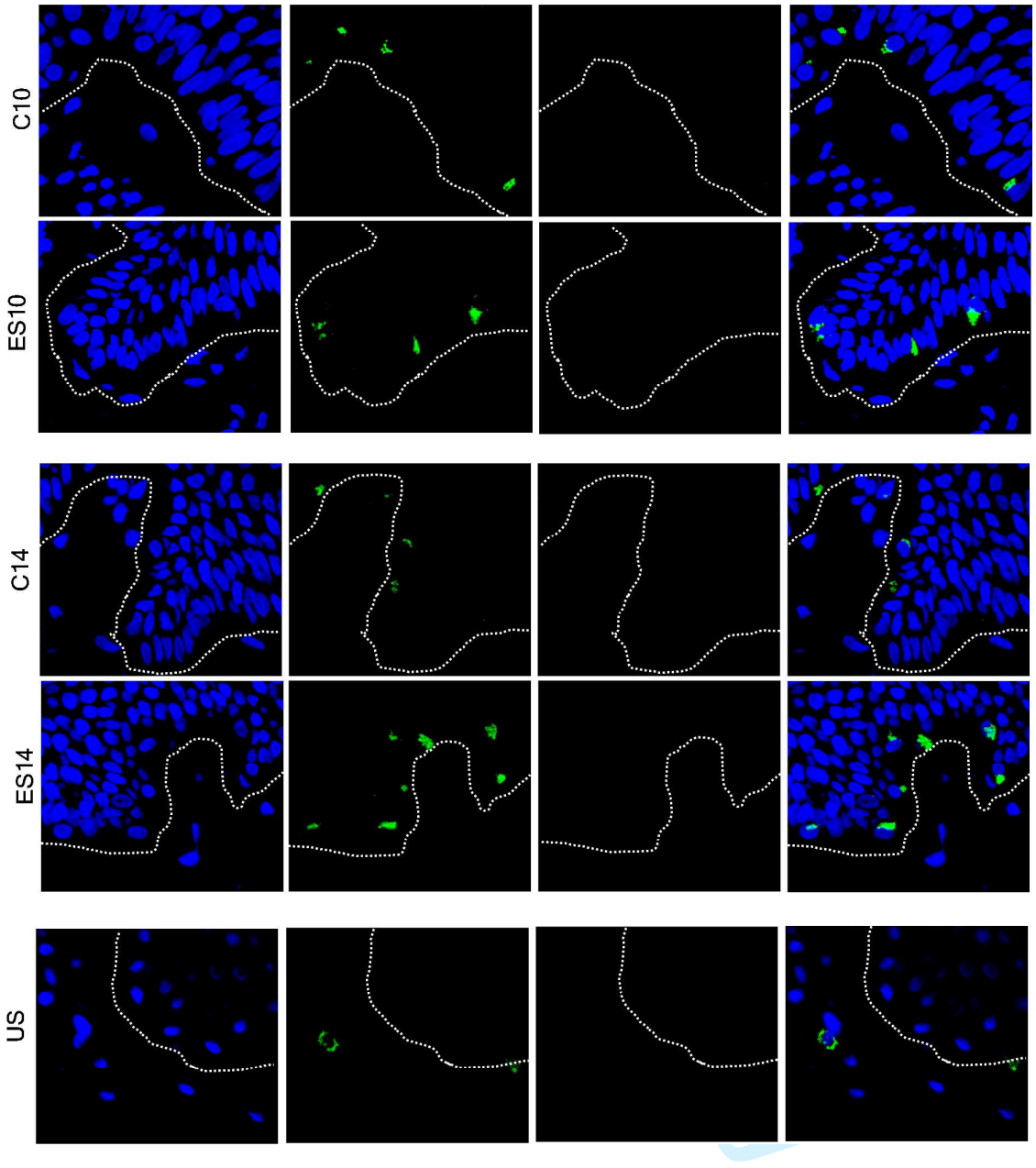

Figure S5. Proliferation analysis of melanocytes in human cutaneous healing normal healing wounds. Ki67/gp100 co-expression analysis showed no significant difference in cellular proliferation between ES-treated and non-ES treated wounds. Dotted lines represent epidermal-dermal junction. US is uninjured skin. Scale bar is 100 μm.

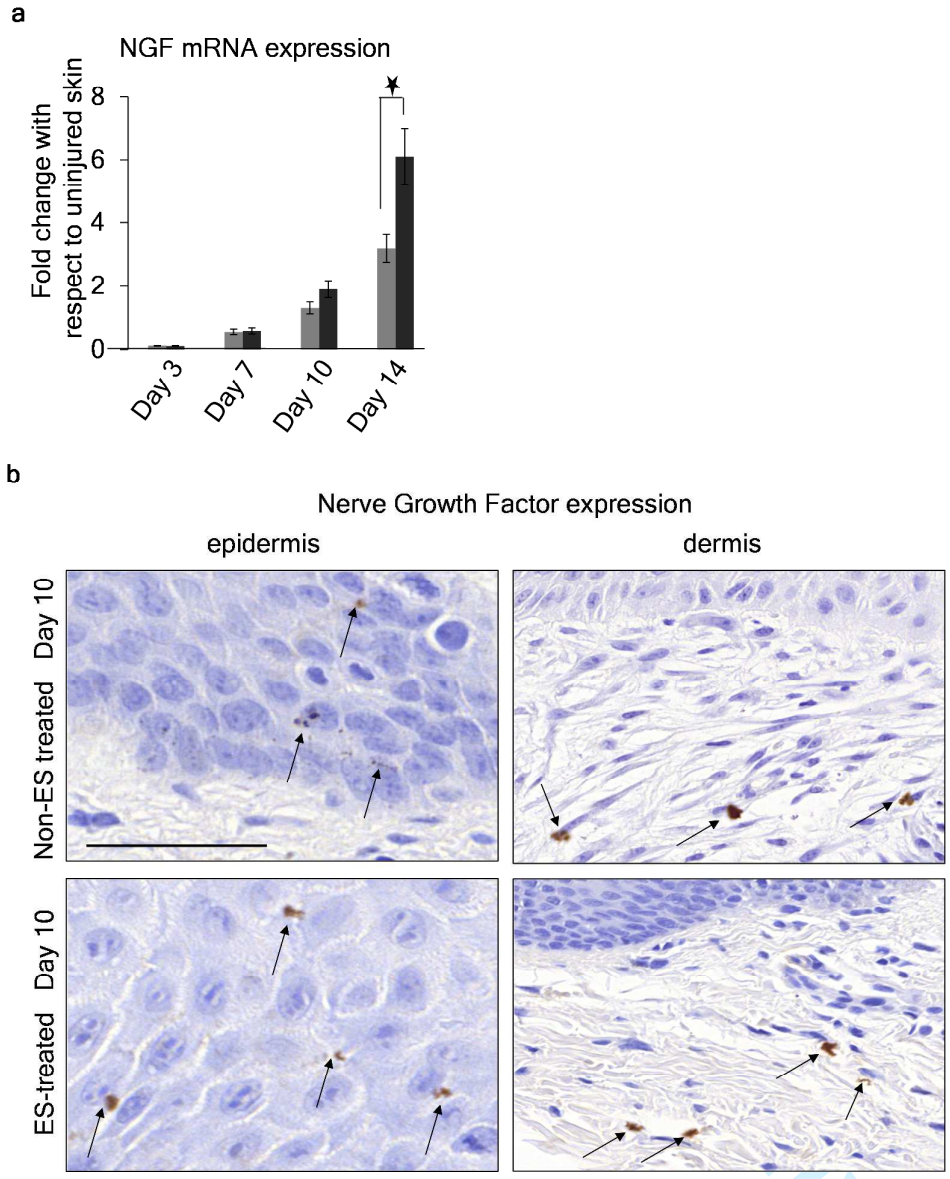

Figure S6: Up-regulated NGF expression in human skin healing by ES. **(a)** qRT-PCR of NGF showed ~ 1.46 and 1.91 fold increase in ES treated wounds compared non-ES treated wounds, on days 10 and 14 respectively. **(b)** NGF protein expression in C10 and ES10 wounds. NGF expression level was significantly lower in all other healing days (before 10) for microscopic observation and further quantitation. Scale bar is 100 μm.

control (non-ES treated) wounds, ES treated wounds.

Indicates statistical significance, $P < 0.05$.

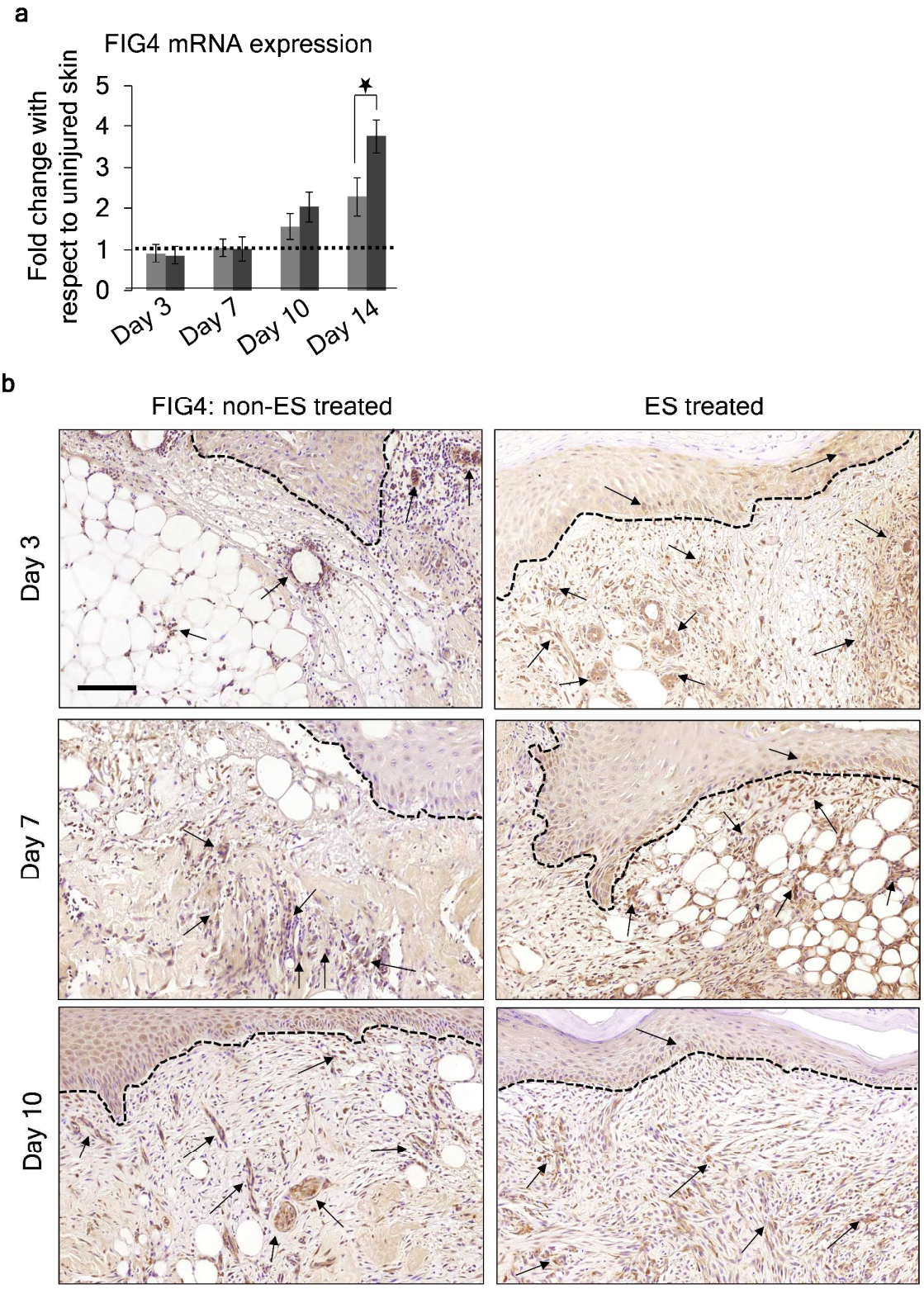
a
FIG4 mRNA expression
Fold change with respect to uninjured skin
0
1
2
3
4
5
Day 3
Day 7
Day 10
Day 14
b
FIG4: non-ES treated
ES treated
Day 3
Day 7
Day 10

Figure S7. ES up-regulates FIG4 expression in healing human skin wounds. (a) qRT-PCR of FIG4 in healing wounds. **(b)** Up-regulated FIG4 expression was observed in ES treated wounds compared to control wounds. In all images, dotted lines indicate epidermal-dermal junction. Scale bar is 100 μm.

control (non-ES treated) wounds, ES treated wounds.

Indicates statistical significance, $P < 0.05$.

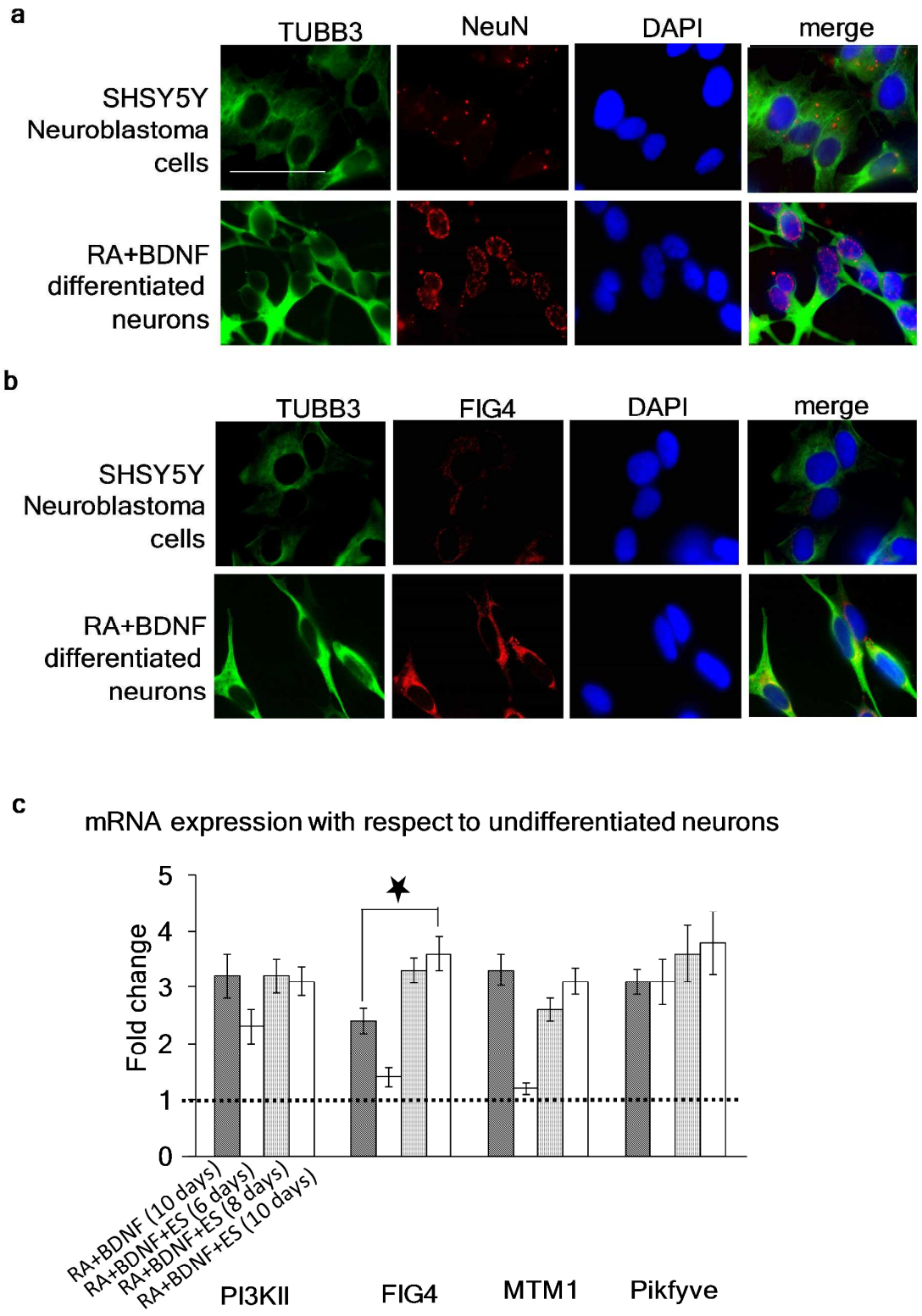
a
TUBB3
NeuN
DAPI
merge
SHSY5Y Neuroblastoma cells
RA+BDNF differentiated neurons
b
TUBB3
FIG4
DAPI
merge
SHSY5Y Neuroblastoma cells
RA+BDNF differentiated neurons
c
mRNA expression with respect to undifferentiated neurons
Fold change
0
1
2
3
4
5
RA+BDNF (10 days)
RA+BDNF+ES (6 days)
RA+BDNF+ES (8 days)
RA+BDNF+ES (10 days)
PI3KII
FIG4
MTM1
Pikfyve

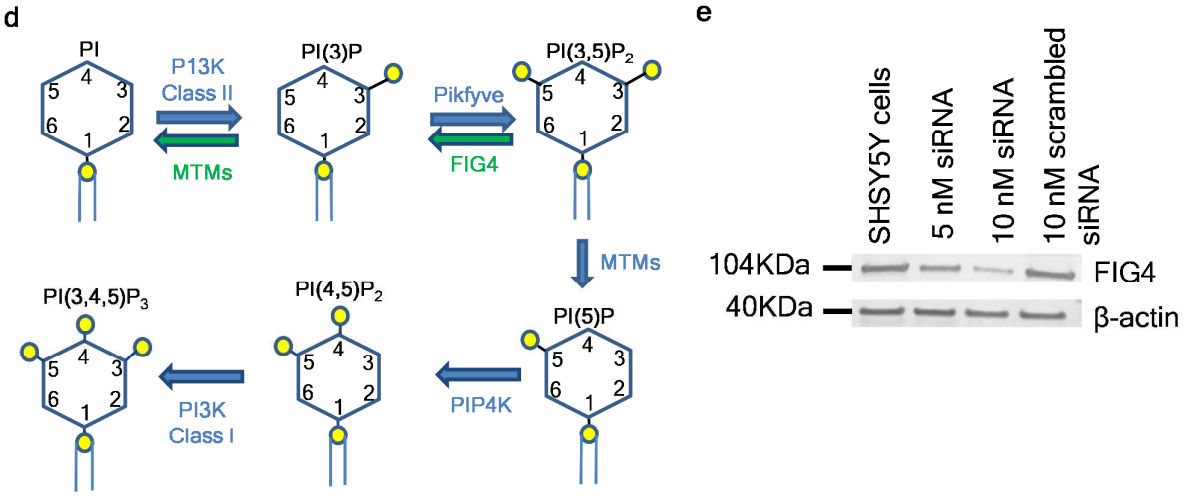
d
PI
P13K
Class II
MTMs
PI(3)P
Pikfyve
FIG4
PI(3,5)P2
MTMs
PI(5)P
PIP4K
PI(4,5)P2
PI3K
Class I
PI(3,4,5)P3

e
SHSY5Y cells
5 nM siRNA
10 nM siRNA
10 nM scrambled siRNA
104KDa
40KDa
FIG4
β-actin

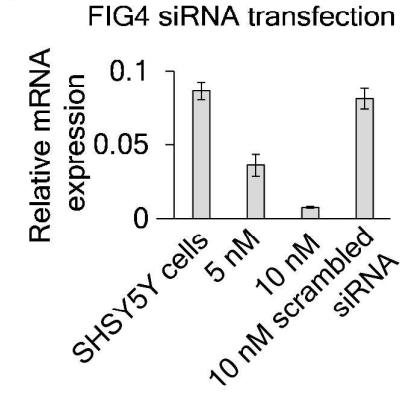
f
FIG4 siRNA transfection
Relative mRNA expression
0.1
0.05
0
SHSY5Y cells
5 nM
10 nM
10 nM scrambled siRNA

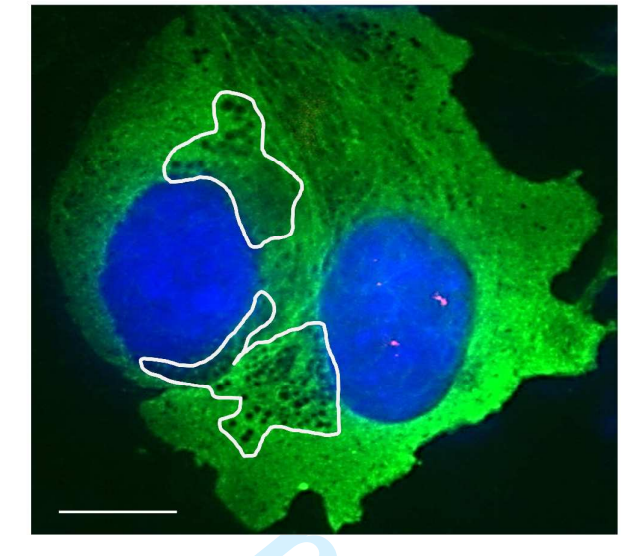
g

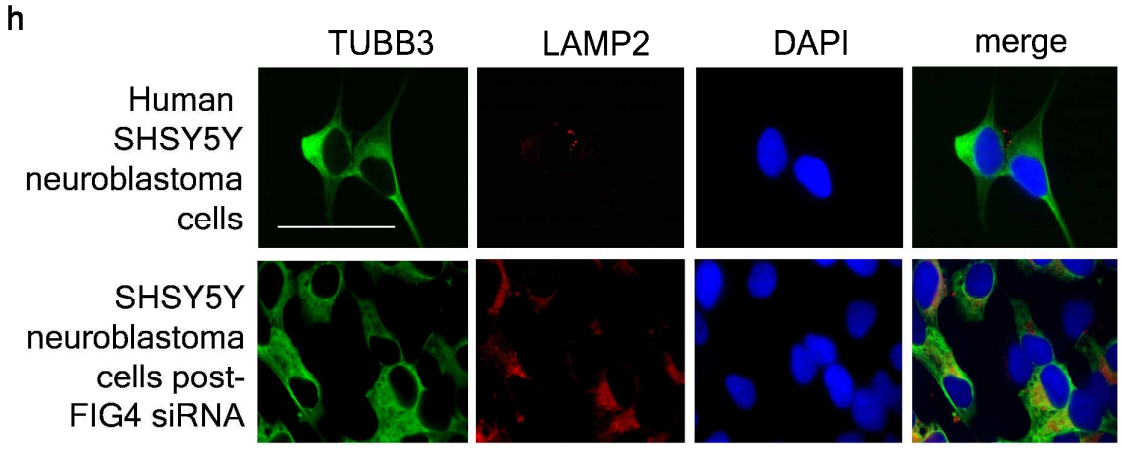
h
TUBB3
LAMP2
DAPI
merge
Human SHSY5Y neuroblastoma cells
SHSY5Y neuroblastoma cells post-FIG4 siRNA

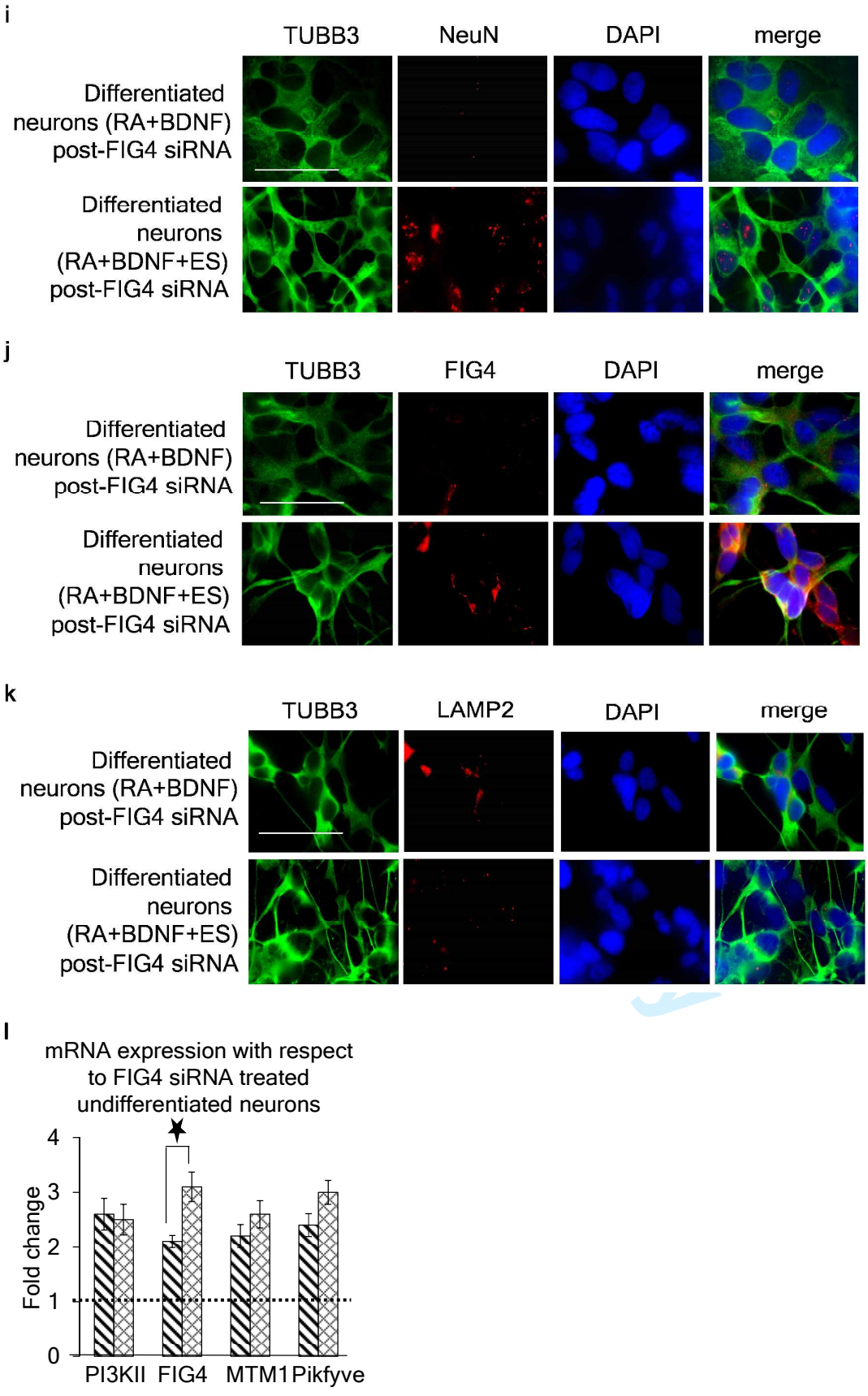
i
TUBB3
NeuN
DAPI
merge
Differentiated neurons (RA+BDNF) post-FIG4 siRNA
Differentiated neurons (RA+BDNF+ES) post-FIG4 siRNA
j
TUBB3
FIG4
DAPI
merge
Differentiated neurons (RA+BDNF) post-FIG4 siRNA
Differentiated neurons (RA+BDNF+ES) post-FIG4 siRNA
k
TUBB3
LAMP2
DAPI
merge
Differentiated neurons (RA+BDNF) post-FIG4 siRNA
Differentiated neurons (RA+BDNF+ES) post-FIG4 siRNA
l
mRNA expression with respect to FIG4 siRNA treated undifferentiated neurons
Fold change
0
1
2
3
4
PI3KII
FIG4
MTM1
Pikfyve

Figure S8. ES enhances human SHSY5Y neuroblastoma differentiation. **(a)** Neuroblastoma cells were differentiated by 'retinoic acid (RA) and brain-derived neurotrophic factor (BDNF)' treatment and the differentiated cells showed up-regulated expression of NeuN. NeuN is a multiply phosphorylated antigen, whose concentration in the nuclei is inversely proportional to chromatin (DNA). **(b)** FIG4 was also up-regulated post-RA+BDNF treatment. **(c)** qRT-PCR post-RA+BDNF+ES treatment and RA+BDNF treatment. Dotted line represents results normalised to undifferentiated cells. **(d)** PIP_3 synthesis pathway. **(e)** SHSY5Y neuroblastoma cells were transfected with FIG4 siRNA (5 nM and 10 nM). Seventy two hours after transfection, proteins were extracted and subjected to Western blot analysis. Successful knock down was achieved at 10 nM concentration of the transfecting siRNA. **(f)** mRNA expression after FIG4 gene knock down. **(g)** Vacuologenesis post-FIG4 siRNA treatment in undifferentiated SHSY5Y cells. Scale bar is 10 μm. **(h)** LAMP2 expression indicating late endosome formation and further leading to vacuole formation in neuroblastoma cells post-FIG4 siRNA treatment. LAMP2 is a marker for late endosome stage. **(i)** Cells subjected to RA+BDNF+ES post-FIG4 siRNA treatment had higher NeuN expression compared to control cells which were not exposed to ES. **(j)** FIG4 was also up-regulated post-ES treatment compared to control cells. **(k)** LAMP2 was decreased in cells subjected to ES post-FIG4 siRNA treatment compared to control cells which were not exposed to ES. **(l)** qRT-PCR post-RA+BDNF+ES treatment and RA+BDNF treatment (both after FIG4 siRNA transfection). Dotted line represents results normalised to undifferentiated cells post FIG4 siRNA treatment. Scale bar is 50 μm (all figures except g).

RA+BDNF treated cells for10 days.

RA+BDNF+ES treated cells for 6 days, for 8 days and for 10 days.

Undifferentiated neurons, RA+BDNF treated cells, RA+BDNF+ES treated cells

✦ Indicates statistical significance, $P < 0.05$.

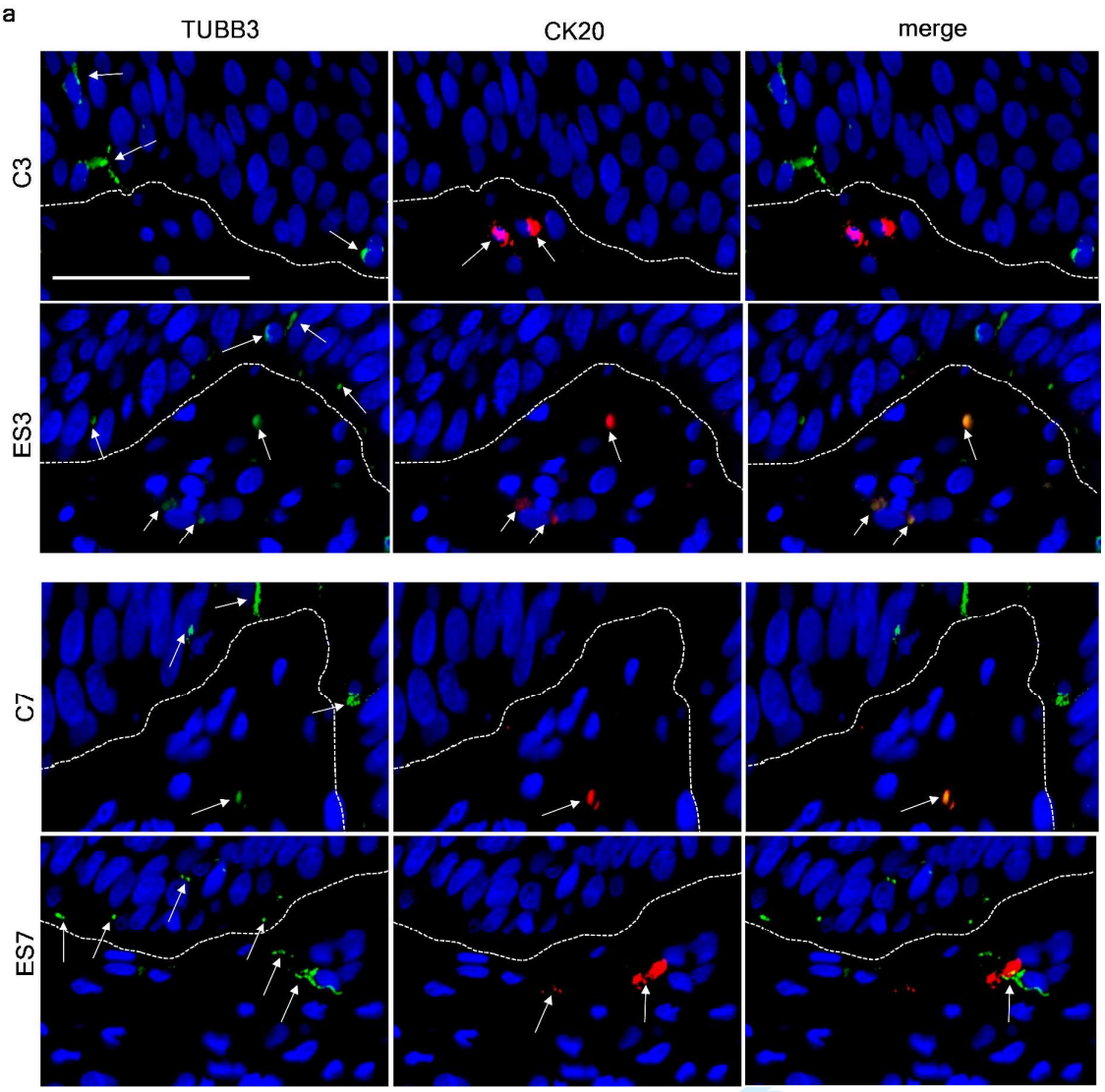
a
TUBB3
CK20
merge
C3
ES3
C7
ES7

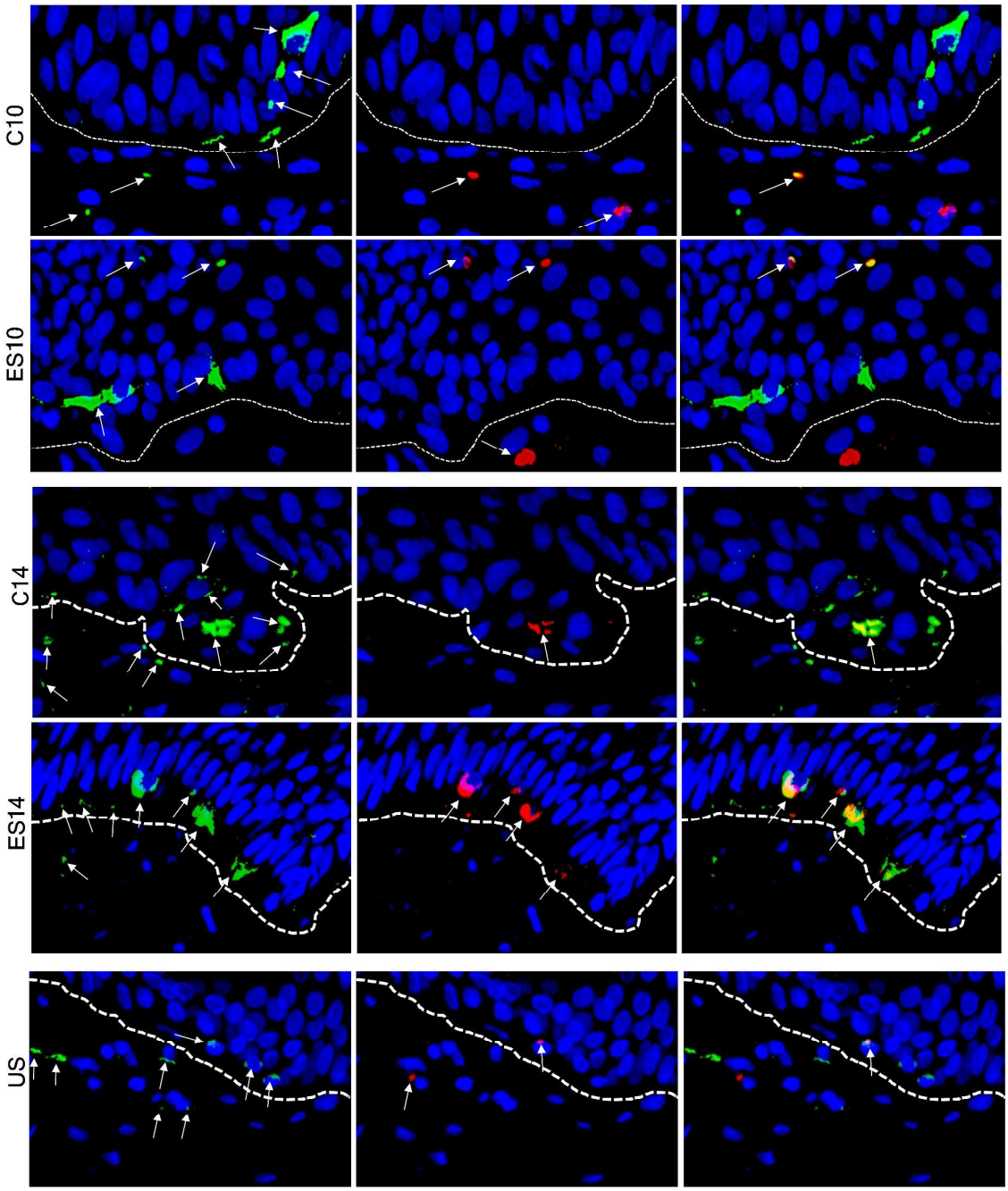
C10
ES10
C14
ES14
US

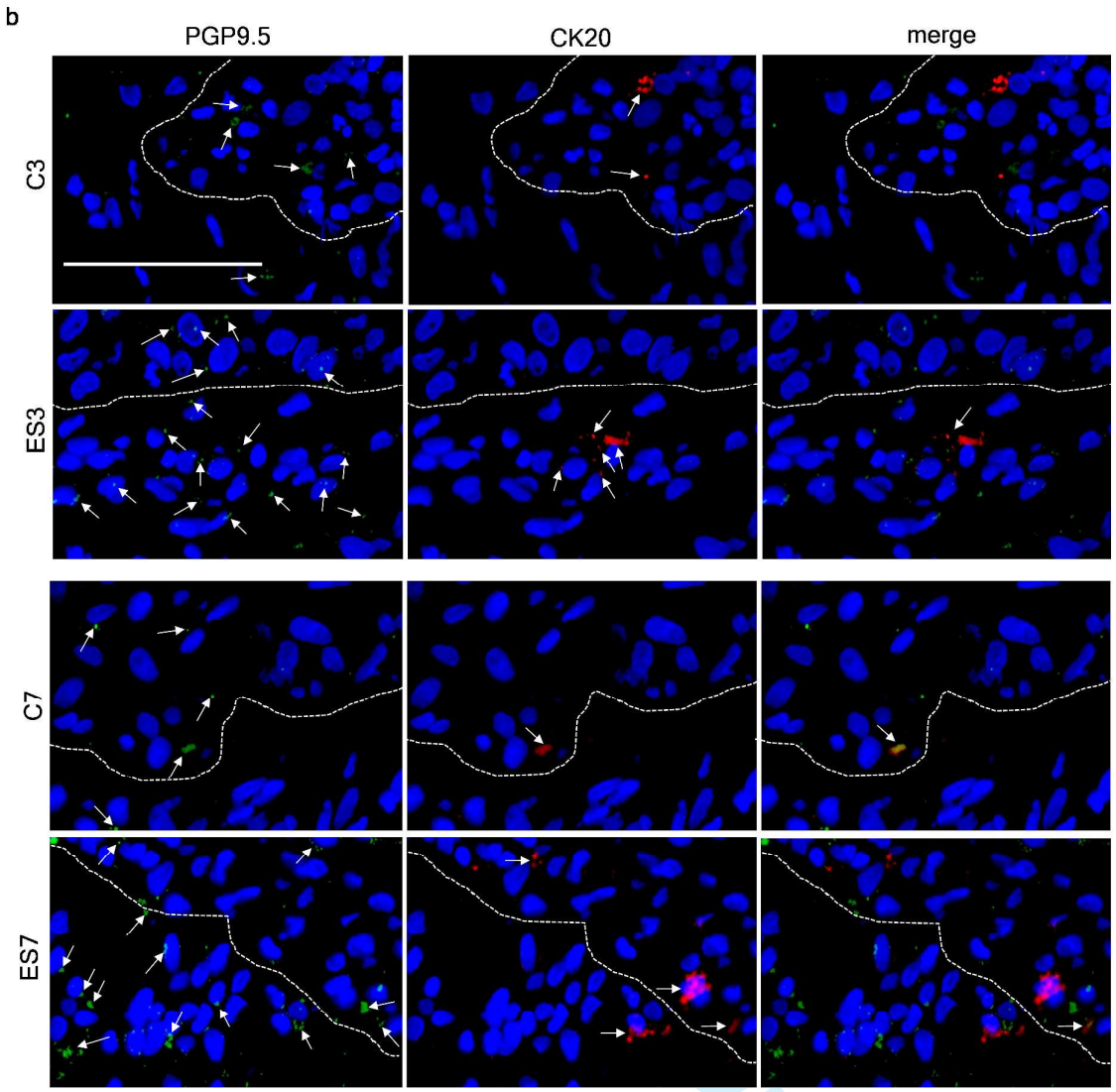
b
PGP9.5
CK20
merge
C3
ES3
C7
ES7

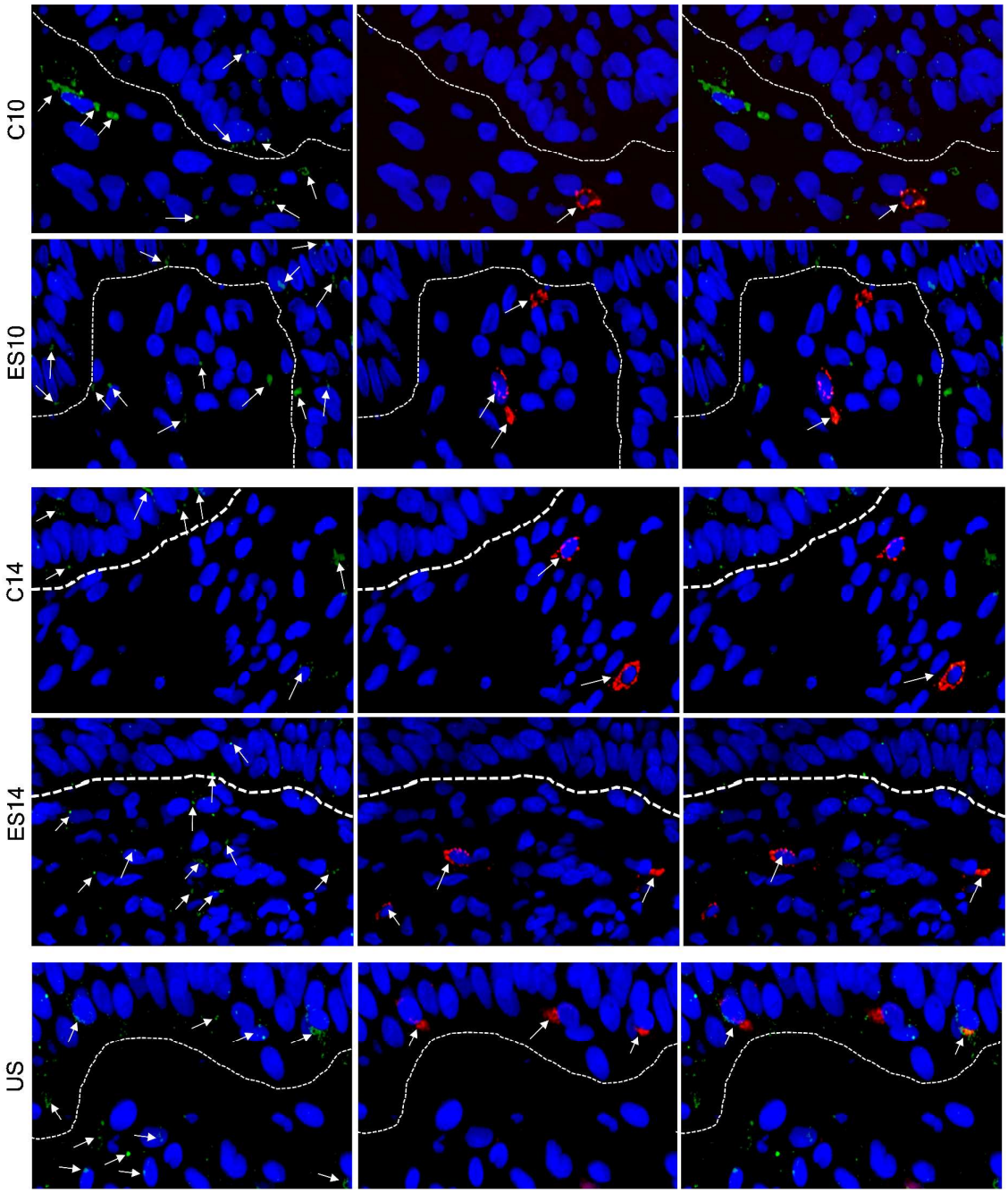
C10
ES10
C14
ES14
US

Figure S9. Up-regulated TUBB3 and PGP9.5 expressions in Merkel cells in ES treated human skin wounds. **(a)** Co-expression of TUBB3/CK20 in human cutaneous wounds undergoing ES and non-ES treated wounds. **(b)** PGP9.5/CK20 co-expression images of ES treated and non-ES treated wounds. Dotted lines indicate epidermal-dermal junction. US is uninjured skin. Scale bar is 100 μm.

Dataset S1: Microarray data comparing uninjured skin (US) to electrically stimulated healing wounds on day 14 (ES14) and control (non-ES treated) wounds on day 14 (C14).

Video S1: Application of ES to human SHSY5Y neuroblastoma cells post-FIG4 siRNA treatment and RA+BDNF differentiation protocol. Cells were subjected to a single course of ES on the final day of RA+BDNF addition. Here, all cells were lysed within 35 minutes of ES.

Video S2: Application of ES to human SHSY5Y neuroblastoma cells post-FIG4 siRNA treatment and RA+BDNF+ES differentiation protocol. To understand the effect of ES during neural differentiation post-FIG4 siRNA treatment, cells were exposed to electric field of 100 mV/mm for 1 hour/day during RA+BDNF differentiation protocol which lasted for 10 days. On the 10^{th} day, cells showed better differentiation phenotype than the non-ES treated cells (RA+BDNF alone) and additionally, survived the entire duration of ES. This indicates the ability of ES to impart integrity to cells.

Supplementary Tables

Table S1. Demographic data of normal human skin used in this study.

Sample number	Sex	Ethnic Background	Age
1	F	British Caucasian	28
2	F	British Caucasian	21
3	M	British Caucasian	20
4	M	British Caucasian	19
5	F	British Caucasian	24
6	F	British Caucasian	30
7	M	British Caucasian	22
8	F	British Caucasian	27
9	F	British Caucasian	24
10	F	British Caucasian	22
11	F	British Caucasian	27
12	F	British Caucasian	30
13	F	British Caucasian	22
14	F	British Caucasian	31
15	**F**	**British Caucasian**	**28**
16	F	British Caucasian	26
17	**M**	**British Caucasian**	**30**
18	F	British Caucasian	30
19	M	British Caucasian	30
20	F	British Caucasian	28
21	F	British Caucasian	26
22	M	British Caucasian	21
23	M	British Caucasian	21
24	M	British Caucasian	19
25	**M**	**British Caucasian**	**28**
26	F	British Caucasian	27
27	F	British Caucasian	22
28	F	British Caucasian	18
29	**F**	**British Caucasian**	**26**
30	F	British Caucasian	21
31	F	British Caucasian	24
32	F	British Caucasian	22
33	F	British Caucasian	20
34	M	British Caucasian	18
35	M	British Caucasian	23
36	F	British Caucasian	21
37	F	British Caucasian	20
38	F	British Caucasian	28
39	F	British Caucasian	21
40	F	British Caucasian	20

Table S2. Details of primers used for qRT-PCR.

Gene	Primers (bp) FP: Forward primer RP: Reverse primer	Accession number	Amplicon product size (bp)
FIG4	FP: gaggtcagaggccctttcat (20) RP: agatgttctccgcattcagc (20)	cat. no. 04687582001	61
MTM1	FP: taaatgcagtggccaacaag (20) RP: aagttcggcgttatgatatgc (21)	cat. no. 04688627001	71
NGF	FP: tccggacccaataacagttt (20) RP: ggacattacgctatgcacctc (21)	cat. no. 04687655001	75
PI3KII	FP: gcaacgagaaagagatgcaa (20) RP: ctcatggatctcggcaatg (19)	cat. no. 04686918001	74
Pikfyve	FP: tccttctggcttcctctgtc (20) RP: ggtagaacaaaacccacacca (21)	cat. no. 04687639001	60
PGP9.5	FP: cctgaagacagagcaaaatgc (21) RP: aaatggaaattcaccttgtcatct (24)	NM_004181.3	110

RPL32	FP: gaagttcctggtccacaacg (20) RP: gagcgatctcggcacagta (19)	NM_000994.3	77
TUBB3	FP: acgtgtgagctgctcctgt (19) RP: aaaaacaaaaccgtaaaacgtca (23)	cat. no. 04684974001	67

Table S3. Primary antibodies, secondary antibodies, concentration of antibodies, incubation parameters and detection methods used for immunocytochemistry and immunohistochemistry analyses.

Primary antibody name, product code and company	Primary antibody raised species, isotype and concentration	Primary antibody incubation details	Secondary antibody, company, concentration, incubation details	Detection method
Cytokeratin 20, ab76126, Abcam, Cambridge, UK	Rabbit (monoclonal), IgG, 1:100 dilution	1 hour, room temperature	Goat anti-rabbit Alexa 546, Molecular probes, Life technologies cat. A11010, 1:200 dilution, (1h room temp)	Fluorescence
			Goat anti-rabbit Alexa 488, Molecular probes, cat. A11034, 1:200 dilution, (1h room temp)	
FIG4, Ab97621, Abcam, Cambridge, UK	Rabbit (polyclonal), IgG, 1:1500 dilution	1 hour, room temperature	Universal antibody by Novolink ™ Leica Biosystems Newcastle ltd, Newcastle Upon Tyne, UK cat. RE7150-K (1h room temp)	Peroxidase
	Rabbit (polyclonal), IgG, 1:250 dilution	4˚C, overnight	Goat anti- Rabbit Alexa 546, Molecular probes, Life technologies ltd, Paisley, UK cat no. A11010, 1:250 dilution, (1h room temp)	Fluorescence

			Goat anti-rabbit Alexa 488, Molecular probes 1:200 dilution, (1h room temp)	
Ki67, ab8191, Abcam, UK	Mouse (monoclonal), IgG1, 1:50	1 hour, room temperature	Goat anti- mouse Alexa 546, Molecular probes, 1:250 dilution, (1h room temp)	Fluorescence
LAMP2 Ab37024, Abcam, UK	Rabbit (polyclonal), IgG, 1:250 dilution	4˚C, overnight	Goat anti- Rabbit Alexa 546, Molecular probes 1:250 dilution, (1h room temp)	Fluorescence
NeuN Ab177487, Abcam, UK	Rabbit (monoclonal), IgG, 1:200 dilution	4˚C, overnight	Goat anti- Rabbit Alexa 546, Molecular probes 1:250 dilution, (1h room temp)	Fluorescence
NGF, Ab6199, Abcam, UK	Rabbit (polyclonal), IgG, 1:250	1 hour, room temperature	Universal antibody by Novolink ™ Leica Biosystems Newcastle ltd, Newcastle Upon Tyne, UK cat. RE7150-K, (1h room temp)	Peroxidase
PGP9.5, ab10404, Abcam, UK	Rabbit (polyclonal), IgG, 1:500 dilution	1 hour, room temperature	Goat anti- rabbit Alexa 546, Molecular probes, 1:250 dilution, (1h room temp) Goat anti-rabbit Alexa 488, Molecular probes, 1:200 dilution, (1h room temp)	Fluorescence
Substance P, ab14184, Abcam, UK	Mouse (monoclonal), IgG1, 1:250	1 hour, room temperature	Goat anti- mouse Alexa 546, Molecular probes, cat. A11003, 1:250 dilution, (1h room temp)	Fluorescence

TUJ-1 (specific for TUBB3), ab14545, Abcam, UK	Mouse (monoclonal), IgG2a, 1:500	1 hour, room temperature	Universal antibody by Novolink ™ (1h room temp)	Peroxidase
		4˚C, overnight	Goat anti- mouse Alexa 488, Molecular probes, cat no.A11001 1:250 dilution, (1h room temp)	Fluorescence

Table S4. Primary antibodies, secondary antibodies, concentration of antibodies, incubation parameters and detection methods used for Western blotting.

Primary antibody name, product code and company	Primary antibody raised species, isotype and concentration	Primary antibody incubation details	Secondary antibody, company, concentration, incubation details	Detection method
β-actin, ab8227, Abcam, UK	Rabbit (polyclonal) IgG, 1:850 dilution	4ºC, overnight	Goat IgG conjugated to alkaline phosphatase, ab97048, Abcam, UK 1:2000 dilution, (1h room temp)	Alkaline phosphatase
FIG4, Ab97621, Abcam, UK	Rabbit (polyclonal), IgG, 1:1500 dilution	4ºC, overnight	Goat IgG conjugated to alkaline phosphatase, ab97048, Abcam, UK 1:2000 dilution, (1h room temp)	Alkaline phosphatase
MTM1 Ab103626, Abcam, UK	Rabbit (monoclonal), IgG,1:1000 dilution	4ºC, overnight	Goat IgG conjugated to alkaline phosphatase, ab97048, Abcam, UK 1:2000 dilution, (1h room temp)	Alkaline phosphatase
NGF, ab6199, Abcam, UK	Rabbit (polyclonal), IgG, 1:500 dilution	4ºC, overnight	Goat IgG conjugated to alkaline phosphatase, ab97048, Abcam, UK 1:2000 dilution, (1h room temp)	Alkaline phosphatase
PGP9.5, ab10404, Abcam, UK	Rabbit (polyclonal), IgG, 1:750 dilution	4ºC, overnight	Goat IgG conjugated to alkaline phosphatase, ab97048, Abcam, UK 1:2000 dilution, (1h room temp)	Alkaline phosphatase
PI3KII, Ab186135, Abcam, UK	Rabbit (polyclonal), IgG, 1:1000 dilution	4ºC, overnight	Goat IgG conjugated to alkaline phosphatase, ab97048, Abcam, UK 1:2000 dilution, (1h room temp)	Alkaline phosphatase
Pikfyve, Ab173448, Abcam, UK	Mouse (polyclonal), IgG, 1:500 dilution	4ºC, overnight	Goat IgG conjugated to alkaline phosphatase, ab97020, Abcam, UK 1:2000 dilution, (1h room temp)	Alkaline phosphatase

Substance P (TAC1), PA5-25766, Thermo scientific, Loughborough, UK	Rabbit (polyclonal), IgG, 1:750 dilution	4ºC, overnight	Goat IgG conjugated to alkaline phosphatase, ab97048, Abcam, UK 1:2000 dilution, (1h room temp)	Alkaline phosphatase
TUJ-1 (specific for TUBB3), ab14545, Abcam, UK	Mouse (monoclonal), IgG2a, 1:750 dilution	4ºC, overnight	Goat IgG conjugated to alkaline phosphatase, ab97020, Abcam, UK 1:2000 dilution, (1h room temp)	Alkaline phosphatase

Supplementary Materials and Methods

SHSY5Y cell culture and differentiation

Human neuroblastoma SHSY5Y cells (ATCC, CRL-2266) were grown in Dulbecco's modified eagle medium with nutrient mixture F12 (DMEM-F12; cat.11320-074; Life Technologies, Paisley, UK) supplemented with 10% fetal calf serum (FCS), 4 x 10^{-3} M glutamine, 10 U/ml penicillin and 10 mg/ml streptomycin. Cells were incubated at 37 °C in a 5% (v/v) CO_2 humidified atmosphere. Cells were seeded on to 22 mm round cover slips (BD Biosciences, Oxford, UK) in 6-well plates (at density of 3 x 10^4 cells/cm^2). After 24 hours, neural differentiation was induced with retinoic acid (RA; 10^{-5} M; cat. R2625, Sigma Aldrich, Dorset, UK) in medium supplemented with 2% FCS for 6 days. Brain derived neurotrophic factor (BDNF; 50 ng/ ml; cat. B3795, Sigma Aldrich, UK) was added for further 4 days in medium supplemented with 0.5% FCS, as previously reported(Mastroeni *et al.*, 2009).

Human punch biopsy collection for wound healing studies

The protocol that we adopted for *in vivo* ES studies is mentioned in our previous study(Sebastian *et al.*, 2015). We divided volunteers into 2 cohorts (n=20 in each cohort); first cohort (Cohort A) providing punch biopsies for normal and ES-treated wound healing on days 3 and 7 and the second cohort (Cohort B) providing for normal and ES-treated wound healing on days 10 and 14. The methodology adopted for both the sets were the same except the days assigned for punch biopsy collection. Normal (control) wound healing biopsies collected on days 3, 7, 10 and 14 are denoted as C3, C7, C10 and C14 respectively. Similarly, ES-treated healing biopsies collected on days 3, 7, 10 and 14 are denoted as ES3, ES7, ES10 and ES14 respectively.

Cohort A

On day 0, participants had two 5 mm diameter full thickness skin biopsies performed under their upper inner arm which acted as the control arm to monitor normal wound healing. On day 3, one 7 mm diameter skin biopsy was performed encompassing one of the previous wound sites (C3). On day 7, another 7 mm diameter skin biopsy was performed to excise the second previous wound site (C7). On Day 7 itself, 2 x 5 mm biopsies were created in the same anatomical location on the contralateral upper inner arm with an intervention phase of ES treatment(Ud-Din *et al.*, 2012). From this day onwards (day 7), the volunteer was treated with ES until day 14. Intermediate biopsies from ES-treated volunteers were taken on days 10 (ES3) and 14 (ES7), similar to that on days 3 (C3) and 7 (C7) for normal healing.

Cohort B

In this cohort, biopsies were collected on days 10 (C10) and 14 (C14) to obtain normal healing samples on days 10 and 14. However, the other 2 biopsies on the contralateral arm were made on day 14. From day 14 onwards, the volunteer was treated with ES and wounds were re-biopsied on days 24 (ES10) and 28 (ES14).

Microarray analysis

In microarray (n=4), normal wound healing samples were compared to ES samples on days 3, 7, 10 and 14. Agilent Whole Human Genome (SurePrint G3 Hmn GE 8x60K V2) Oligo Microarray kit (Agilent Technologies) was used in this study following the manufacturer's protocol—One-Color Microarray-Based Gene Expression Analysis (Low Input QuickAmp

Labeling kit)(Shih *et al.*, 2012). Data was analyzed with Qlucore Omics Explorer (Qlucore AB, Lund, Sweden)(Larsen. *et al.*, 2013). Statistical significance ($P < 0.05$) was also generated by the same software.

Immunohistochemistry and immunocytochemistry

For tissue immunofluorescence experiments, dewaxing and antigen retrieval were performed as explained earlier. Further, tissues were permeabilised with 0.2% Triton X-100 in PBS for 30 min and later blocked with 5% bovine serum albumin in PBS. They were later stained with appropriate primary and secondary antibodies, and co-stained with 4',6-diamidino-2-phenylindole (DAPI; cat. H-1200, Vector Laboratories, Burlingame, CA, USA).

For immunocytochemistry experiments, cells were fixed with 4% paraformaldehyde for 20 min, permeabilised with 0.2% Triton X-100 in PBS for 30 min. They were blocked with 5% bovine serum albumin in PBS for 1 hour. Cells were then stained with appropriate primary and secondary antibodies, and co-stained with DAPI.

All antibodies and incubation parameters are detailed in Supplementary Table S3.

Immunohistochemistry image analysis by Definiens software

Definiens tissue studio version 3.51 (Definiens AK, Munchen, Germany) was used to quantitate the IHC results(Sebastian *et al.*, 2015). The slides were scanned and images were uploaded on Definiens IHC software to further quantitate the results. Here, initially, in the cellular analysis module, 12 subsets were selected in the tissue specimen for site recognition. Nuclear detection, nuclear area detection and nucleus classification were also done on the

subsets. For IHC-peroxidase staining, hematoxylin threshold was adjusted for cell detection. Analysis was done in 20X magnification.

Western blot band analysis by Image J software

Percentage of band intensity was calculated by Image J (Fiji, 1.47t, NIH, USA) analysis(Sebastian *et al.*, 2015). Band intensity was calculated in the software by assessing profile plot of bands, followed by analysing and labelling the generated peaks. This band intensity was then normalised to the respective β-actin band. Then the percentage was calculated based on the intensity of the normalised individual bands compared to the total intensity of the rest of the bands in the particular row (for the particular protein), which were calculated accordingly.

Masson-Fontana histochemistry

Briefly, 4-µm thick sections were cut from paraffinized tissue blocks. They were dewaxed in a series of xylene and ethanol. Antigen retrieval was done with citrate buffer (pH 6.0) at 60˚C for 1 h. Tissues were treated with ammoniacal silver nitrate solution (10% silver nitrate (cat. 209139; Sigma-Aldrich) + conc. ammonium hydroxide (cat. 320145; Sigma-Aldrich) added drop-wise until it turns clear, leave 24 hours in dark at room temperature) for 40 min at 56℃ in the dark. After washing in distilled water, the sections were treated with 5% aqueous sodium thiosulphate (cat. 72049; Sigma-Aldrich) for 1 min. Then the sections were washed in running tap water for 3 min and counterstained with haematoxylin for 3 min. After washing in distilled water, sections were dehydrated and coverslipped.

Microscopy and nerve fibre thickness

Live-cell imaging was performed using an inverted Olympus IX71 microscope (Olympus, Southend-on-sea, UK) with a 20X NA objective. Fluorescence images were taken using an upright Olympus IX51 microscope (Olympus, UK) with a 100X oil immersion objective. The average fibre thickness was determined by taking 12 measurements/sample randomly from the fibre network and analysing in NIH Image J software.

References

Larsen. MJ, A.Kruse T, Laenkholm A-V, Bak M, E.Lykkesfeldt A, P.Sörensen K, *et al.* (2013) Classifications within Molecular Subtypes Enables Identification of BRCA1/BRCA2 Mutation Carriers by RNA Tumor Profiling. *PloS one* 8.

Mastroeni D, Grover A, Leonard B, Joyce JN, Coleman PD, Kozik B, *et al.* (2009) Microglial responses to dopamine in a cell culture model of Parkinson's disease. *Neurobiology of aging* 30:1805-17.

Sebastian A, Iqbal SA, Colthurst J, Volk SW, Bayat A (2015) Electrical Stimulation Enhances Epidermal Proliferation in Human Cutaneous Wounds by Modulating p53-SIVA1 Interaction. *The Journal of investigative dermatology*.

Shih B, Sultan MJ, Chaudhry IH, Tan KT, Johal KS, Marstan A, *et al.* (2012) Identification of biomarkers in sequential biopsies of patients with chronic wounds receiving simultaneous acute wounds: a genetic, histological, and noninvasive imaging study. *Wound repair and regeneration : official publication of the Wound Healing Society [and] the European Tissue Repair Society* 20:757-69.

Ud-Din S, Perry D, Giddings P, Colthurst J, Zaman K, Cotton S, *et al.* (2012) Electrical stimulation increases blood flow and haemoglobin levels in acute cutaneous wounds without affecting wound closure time: evidenced by non-invasive assessment of temporal biopsy wounds in human volunteers. *Experimental dermatology* 21:758-64.